frontiers | Frontiers in Nanotechnology

TYPE Review
PUBLISHED 16 August 2024
DOI 10.3389/fnano.2024.1433591



OPEN ACCESS

EDITED BY
Chella Santhosh,
K L University, India

REVIEWED BY
Ramachandran Balaji,
K L University, India
Bhanu Chandra Marepally,
Chaitanya Bharathi Institute of Technology, India

*CORRESPONDENCE
Anindita Chatterjee,
anindita.chemistry@gmail.com

RECEIVED 16 May 2024
ACCEPTED 22 July 2024
PUBLISHED 16 August 2024

CITATION
Chatterjee A, Kumar GK, Roymahapatra G, Das HS, Jaishree G and Rao TS (2024) Zinc chalcogenide nanostructures: synthesis methodologies and applications—a review. *Front. Nanotechnol.* 6:1433591. doi: 10.3389/fnano.2024.1433591



# Zinc chalcogenide nanostructures: synthesis methodologies and applications—a review

Anindita Chatterjee [1]*, G. Kiran Kumar [2], Gourisankar Roymahapatra [3], Himadri Sekhar Das [4], G. Jaishree [1] and T. Siva Rao [5]

[1]Department of Chemistry, Raghu Engineering College, Visakhapatnam, India, [2]Department of Physics, Raghu Engineering College, Visakhapatnam, India, [3]Department of Applied Sciences, Haldia Institute of Technology, Haldia, India, [4]Department of Electronics and Communication Engineering, Haldia Institute of Technology, Haldia, India, [5]Department of Chemistry, Andhra University, Visakhapatnam, India

Zinc chalcogenide nanostructures are an important class of non-toxic nanomaterials due to their biocompatible nature, surface flexibility, high degree of crystallinity, and high photoluminescence efficiency that makes them applicable in solar cells biosensors, photocatalysts, LEDs, and electroluminescence materials. There are various methods for synthesizing zinc chalcogenides, including ZnS, ZnSe, and ZnTe, through colloidal, hydrothermal, solvothermal, microwave, and core shell synthesis to prepare highly luminescent material for drug delivery and biomedical applications. The main focus of this review is to explore various synthetic approaches to tune the morphology, size, and surface properties of zinc-based chalcogenide nanostructures, revealing their potential as biocompatible quantum dots. Despite their advantages, zinc chalcogenides also have certain drawbacks, such as low mechanical strength, limited bandgap tunability, and less thermal stability, that can point the way for future research. Thus, this review may prove beneficial for developing and designing more advanced nanomaterials based on existing knowledge, protocols, and strategies.

KEYWORDS

**zinc chalcogenides, nanostructures, quantum dots, nanoparticles, biocompatible, nontoxic**

## 1 Introduction

Semiconductor quantum dots (QDs) and nanoparticles, typically ranging from 1 to 5 nm in size, possess unique optical and electronic properties resulting from the quantum confinement effect that distinguishes them from larger particles. Quantum dots, often likened to artificial atoms, reveal their unique nature with discrete electronic states similar to those found in natural atoms or molecules (Biju et al., 2008; Mussa Farkhani and Valizadeh, 2014). They have garnered significant interest across various fields, including the material sciences and medicine. Quantum dots are known for applications in bio-labeling, bio-imaging, and sensing (Gao et al., 2004; Medintz et al., 2005; Michalet et al., 2005; Sapsford et al., 2006; Smith et al., 2008; Gao et al., 2010; Park et al., 2011), highlighting their singular nature. Among all semiconductor quantum dot materials, zinc chalcogenide (fundamentally sulfides, selenides, and tellurides) nanostructures stand out as promising

candidates for replacing other metal chalcogenides owing to their confinement of electrons, biocompatibility, and size-dependent photoemission characteristics.

Earlier research on the nanoparticles of semiconductors primarily focused on chalcogenides of cadmium (CdS, CdSe, CdTe) (Priyam et al., 2005; Chatterjee et al., 2006; Chatterjee et al., 2007a; Priyam et al., 2009). However, zinc has recently replaced cadmium due to its lower toxicity (Chatterjee et al., 2021), biocompatibility, and UV absorption properties. Zinc, a harder Lewis acid than cadmium, exhibits differences in ligand affinity, leading to different reaction rates for similar types of precursors of zinc and cadmium compounds. As the smallest atom in the second column of the periodic table, zinc chalcogenides demonstrate stronger bonding among II–VI compounds, along with higher energy gaps, enthalpies of formation, and melting points. These materials absorb UV light and may be engineered to emit in the ultraviolet or near-blue region. Additionally, zinc nanocrystals serve as exceptional host materials for transition metal dopants. This review highlights the synthesis, properties, and numerous applications of zinc chalcogenides (Scheme 1).

## 2 Versatile properties of zinc chalcogenides

Zinc chalcogenides, including zinc sulfide (ZnS), zinc selenide (ZnSe), and zinc telluride (ZnTe), boast numerous significant properties, making them invaluable in optical and optoelectronic devices such as LEDs, photodetectors, and solar cells (Scheme1). Their tunable bandgaps and high optical absorption coefficients enable efficient energy conversion and light emission. ZnS, with its wide bandgap of 3.68–3.91 eV, is ideal for ultraviolet and blue-light emission, while ZnSe, with a bandgap of 2.70 eV, is widely used in infrared optics due to its transparency in the mid- and far-infrared regions. ZnTe, featuring a bandgap of 2.26 eV, finds applications in thin-film transistors, photovoltaic devices, and infrared detectors thanks to its favorable electronic properties and compatibility with existing semiconductor technologies. Additionally, zinc chalcogenide-based nanoparticles can be functionalized for diagnostic applications in cancer detection and drug delivery. With densities ranging from 4.09 g/cm$^3$ for ZnS to 6.34 g/cm$^3$ for ZnTe and melting points from 1,290 °C for ZnTe to 1,850 °C for ZnS, these materials also exhibit increasing refractive indices and dielectric constants. The diverse properties and applications of zinc chalcogenides drive research and innovation in fields ranging from electronics and photonics to environmental monitoring and healthcare, underscoring their essential role in advanced technological solutions.

## 3 Synthesis of zinc chalcogenide nanostructures

Zinc chalcogenide nanoparticles comprising ZnS, ZnSe, and ZnTe are widely researched, with ZnS being particularly prevalent in various applications. These compound semiconductors exhibit remarkable properties suitable for uses diverse as electroluminescence, electrocatalysis, light-emitting diodes (LEDs), and biosensors (Chatterjee et al., 2012; Chatterjee et al., 2021). ZnS is known for its chemical stability and superior technological characteristics compared to other chalcogenides. It exists in two crystalline forms, zinc blende (sphalerite) and wurtzite, and possesses a relatively large difference between valence band and conduction gap of 3.5–3.8 eV. This large bandgap makes ZnS well-suited for devices that utilize visible and UV light. Various synthesis methods, including solid-phase reactions (Kaito et al., 1987), sol-gel processes (Stanić et al., 1997), solvothermal routes (Yu et al., 1998), colloid chemical techniques (Chatterjee et al., 2007b), sonochemicals (Routkevitch et al., 1996; Zhu et al., 2000), liquid phase chemical precipitation (Duan et al., 2003), ion complex transformation methods (Bredol and Merikhi, 1998), and microwave irradiation (Yin et al., 2004), have been employed to produce Zn-chalcogenide nanoparticles which find applications in numerous optoelectronic devices.

### 3.1 Effect of capping agents, reaction temperature, and reactant concentration

The synthesis of zinc chalcogenides involves various parameters that significantly influence the properties and quality of the nanoparticles. The effect of capping agents, reaction temperature, and reactant concentration has been examined by various researchers. Capping agents are crucial in controlling the size, shape, and surface properties of Zn-chalcogenide nanoparticles. These bind to the surface of the nanoparticles, preventing uncontrolled growth and agglomeration. Capping agents can be organic molecules, polymers, or surfactants. Common capping agents include thiols, amines, phosphines, and carboxylic acids. They influence the colloidal stability, solubility, and surface reactivity of the nanoparticles. Different capping agents can result in various nanoparticle shapes (spherical, rod-like, etc.) due to their distinct binding affinities and steric effects. The size distribution of nanoparticles can be finely tuned by selecting appropriate capping agents. The choice of capping agent can provide specific functional groups (Chatterjee et al., 2007b) on the nanoparticle surface, facilitating further modification or functionalization for specific applications.

Similarly, reaction temperature is a critical factor in determining the kinetics of nucleation and growth of Zn-chalcogenide nanoparticles. Higher temperatures generally increase the rate of nucleation and growth, leading to faster synthesis processes. However, excessively high temperatures can lead to uncontrolled growth and larger particle sizes.

The concentration of reactants (Zn precursor and chalcogen source) plays a significant role in the synthesis process, affecting the supersaturation level and growth dynamics of the nanoparticles. High reactant concentrations lead to higher supersaturation, promoting rapid nucleation and the formation of numerous small nuclei. Low reactant concentrations result in fewer nucleation sites and larger particles due to slower growth rates. Higher concentrations typically yield smaller and more uniform nanoparticles, as the increased number of nucleation sites limits the growth of each individual particle. Conversely, lower concentrations may produce larger particles with broader size distributions. The

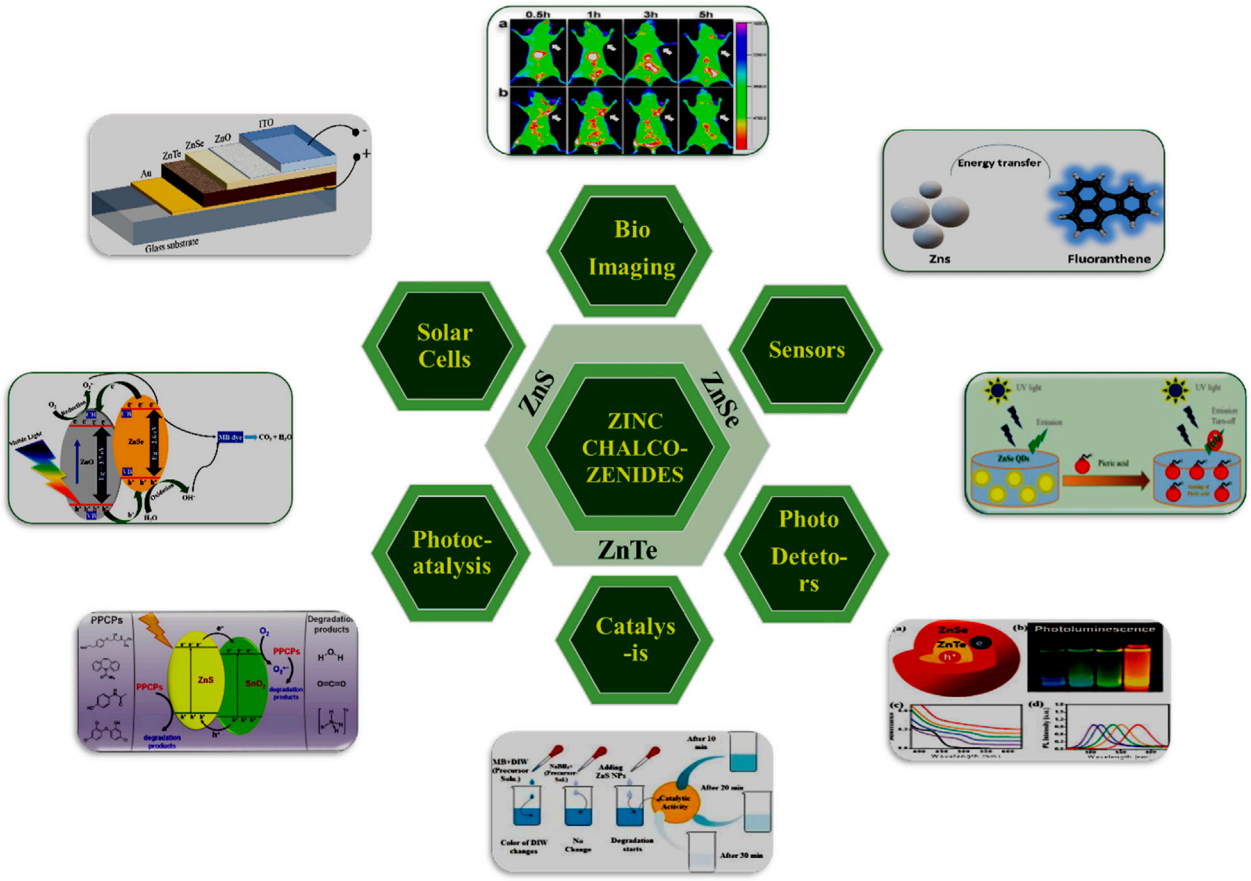


SCHEME 1
Graphical representation of zinc-chalcogenides nanostructures employed in numerous applications.

ratio of zinc precursor to chalcogen source can affect the stoichiometry and composition of the final zinc chalcogenide product. Precise control over reactant concentration is essential for achieving the desired stoichiometry and minimizing defects. The interplay between capping agents, temperature, and reactant concentration is crucial. Adjusting reactant concentrations in the presence of a particular capping agent can further refine the size distribution and surface properties of the nanoparticles.

## 3.2 Synthesis of sulfur-based zinc chalcogenide nanostructures

ZnS nanoparticles (6–12 nm) were first synthesized by the team of J.C. Sanchez-Lopez and E.P. Reddy (Sánchez-López et al., 1999). The average mean diameter of prepared nanoparticles was 8 nm. They described that, with changing reaction conditions, they successfully obtained a homogeneous distribution of the desired ZnS nanostructures in a sphalerite phase.

Soon after, Wang and Hong (2000) introduced a novel solid-state method to produce ZnS nanoparticles using zinc acetate and thioacetamide. The reaction temperature ranged from room temperature to 300 °C. Their method involved thoroughly mixing and milling precise amounts of zinc acetate and thioacetamide powders. Subsequently, the mixed powder was heated to 300 °C in an oven. The resulting product exhibited a pure zinc-blende crystal structure, confirming the formation of ZnS nanoparticles. They reported achieving the size variation of ZnS nanoparticles simply by adjusting the temperature of the reaction in the solid-state method.

In 2003, Ling et al. (Wageh et al., 2003) prepared ZnS quantum dots via a colloidal synthesis using mercaptoacetic acid as the surface capping group. At first, zinc acetate and mercaptoacetic acid were taken in a solvent-like dimethylformamide (DMF), and the medium pH was adjusted to 8. Subsequently, a sodium sulfide solution was added to the reaction mixture under a $N_2$ atmosphere. They studied the characteristic features of luminescence spectra and points defect by varying the refluxing time. On the other hand, Lu et al. (2004) reported the low temperature synthesis of ZnS nanoparticles by reaction with zinc acetate and thioacetamide (TAA). This resulted in the formation of cubic nanocrystals of zinc sulfide with 26 times stronger photoluminescence intensity than ZnS nanoparticles and nanowires.

Moon et al. (2006) developed ZnS nanowires through a chemical vapor transport and condensation method. A gold-coated substrate of silicon was used to grow the nanowires by a reaction of zinc oxide and iron sulfide powder. They used FeS powder as a stable sulfur source and utilized ZnO as a possible desulfurization reagent. Alternatively, a simple chemical vapor transport–condensation (CVTC) technique was employed to grow ZnS nanowires on

gold-coated silicon substrate (Xia et al., 2003). The liquid gold nanodroplets were formed on the surface, and as the temperature increased, gold–ZnS alloys formed by the absorption of ZnS nanodrops by gold. Finally, ZnS nanowires were collected from the precipitates (Jiang et al., 2003; Kar et al., 2005).

Spherical quantum dots of ZnS nanoparticles 3 nm in diameter were prepared by Chatterjee et al. (2007b) (22) through wet colloidal synthesis. The capping agents used were water soluble thiols of cysteine and mercaptoethanol. The growth rate (dr/dt) of the nanoparticles were measured at a constant temperature and heating rate. The colloidal quantum dots obtained were investigated with TEM and XRD and were found to be cubic crystalline in structure and highly photoluminescent in nature. This indicates a valuable significance in synthesizing fluorescent nanomaterials (Chatterjee et al., 2007b) which shows absorbance in the visible range (Figures 1 and 2).

Anand et al. (2009) reported the hydrothermal synthesis of zinc sulfide nanoparticles using hexamethylenetetramine (HMTA) as a surfactant. Zinc acetate dihydrate, thiosemicarbazide, hexamethylenetetramine, and sodium hydroxide along with deionized water were put into a Teflon autoclave chamber and heated for 8 h at 180 °C. This study revealed the dependence of structural and optical properties on the nature of the surfactant in the hydrothermal method for synthesizing chalcogenides.

In 2013, K. Senthil Kumar and K. Ramamurthi reported a low temperature synthesis of MPA-capped ZnS quantum dots using zinc nitrate, sodium sulfide, MPA (3-mercapto propionic acid), and tetrapropylammonium hydroxide (Senthilkumar et al., 2013). They added MPA solution dropwise into the zinc nitrate solution with the subsequent addition of tetrapropylammonium hydroxide to maintain pH 12, followed by the rapid addition of $Na_2S$ solution. The ZnS QDs suspension obtained was clear and colorless, exhibiting a cubic zinc blende structure having a quantum yield almost 31%. They also reported that the emission intensity of synthesized ZnS QDs could be strongly affected by pH.

Bochev and Yordanov (2014) reported the room temperature synthesis of thiol-capped nano zinc sulfide dispersed in water using ZnS, thioglycolic acid, sodium sulfide, and sodium hydroxide. In their approach, the synthesis of ZnS nanoparticles was considered in studying the change in optical characteristics on the precursor concentration and molar ratio of the reactants. The synthesized nanoparticles possess a cubic crystal arrangement and spheroid shape (Figure 3).

In 2015, Senapati and Sarkar (2015) prepared ZnS nanoparticles using a new green chemical approach, employing starch as a capping agent. Starch molecules play a crucial role in the structural modification of composite nanomaterials. Due to presence of anhydrous glucose units previous, ZnS nanoparticles were potentially obtained as cubic crystal structures. Senapati and Sarkar (2015) observed that the energy bandgap values obtained from absorption studies increased with increasing starch concentration.

ZnS thin films were reported by spray pyrolysis (Nithyaprakash et al., 2009; HusseinP, 2013; Lin et al., 2015) in 2015, and the synthesis of ZnS by thermal decomposition, which has single source precursor (Jen-La Plante et al., 2010; Onwudiwe and Ajibade, 2011), has been investigated. In this approach, zinc chloride was added to a solution of ethanol, carbon disulfide, potassium hydroxide, and a secondary amine. They reported the formation of two basic structures of cubic zinc blende (ZB) phase at a low temperature and wurtzite (WZ) phase at high temperature of synthesized ZnS (Kole and Kumbhakar, 2012). They also investigated bandgap and morphological change in structure as the effect of heat treatment at different calcination times of zinc sulfide.

Balavijayalakshmi and Manju (2016) synthesized copper-doped zinc sulfide with various concentrations using wet chemical co-precipitation. They added sodium sulfide solution dropwise into a solution containing cupric chloride and zinc chloride. The resulting mixture was left for 24 h, then centrifuged and heated for 1 h at 160 °C in a hot air oven. The synthesized ZnS was collected in powdered form, and X-ray diffraction analysis revealed a cubic zinc blende pattern. They also observed variation in the bandgap energy, mainly due to the addition of different dopant concentrations, resulting in variations in crystallite size.

In 2018, the team of Q. Alijani and Pourseyedi reported a biogenic method for synthesizing ZnS by leveraging the plant secondary metabolites of *Stevia rebaudiana* (Alijani et al., 2019). They prepared *S. rebaudiana* leaves extract in a flask, shaking it at 90 rpm and 37 °C. The resulting mixture was separated by centrifugation followed by the gradual addition of $Zn(NO_3)_2$ solution with continuous stirring. Water extract of *Stevia* and $Na_2S$ were then added to the solution, which was incubated at 70 °C, resulting in the formation of ZnS nanoparticles. XRD spectrum analysis confirmed that the ZnS nanoparticles belonged to a cubic structure (Dhas et al., 1999; Labiadh et al., 2016; Tran et al., 2016; Sharifi et al., 2018). According to their findings, the size of biosynthesized nanoparticles could be controlled by the ion source, adjusting the plant extract's concentration, pH, and temperature.

In 2018, Y. Wang and colleagues reported on the one-pot aqueous-phase synthesis of ZnS quantum dots co-capped by two surfactant molecules, L-cysteine and mercaptopropionic acid, showing dual emission characteristics (Ren et al., 2018). In their method, both capping agents (cysteine and MPA) were added to a zinc acetate solution while maintaining the solution's pH at 12 through the addition of NaOH. $Na_2S$ solution was then added slowly at 100 °C for 1 h to obtain ZnS QDs, which were purified by water extraction and ethanol precipitation and were found to have a cubic structure. The researchers observed the novel nature of the pure ZnS QDs' strong emission intensity, including dual emissions, which could be accustomed by modifying the molar ratio of cysteine to MPA.

More recently, advanced synthetic methodologies such as colloidal, hydrothermal, solvothermal, microwave, and core-shell synthesis, have been explored to improve the properties and applications of ZnS nanostructures. For example, Ebrahimi and Yarmand (2019) utilized a solvothermal method to produce ZnS nanoparticles with enhanced photoluminescence, demonstrating their potential in optoelectronic applications. Furthermore, Jubeer et al. (2021) highlighted the use of microwave-assisted synthesis to achieve the rapid and efficient production of ZnS nanostructures with controlled morphology and size, enhancing their applicability in bioimaging and photocatalysis. Liu and Li (2018) synthesized ZnS nanocrystals using a hot-injection method, which allowed precise control over particle size and shape. This method involved injecting a sulfur precursor into a hot solution of zinc precursor, resulting in monodisperse ZnS nanocrystals with high crystallinity and

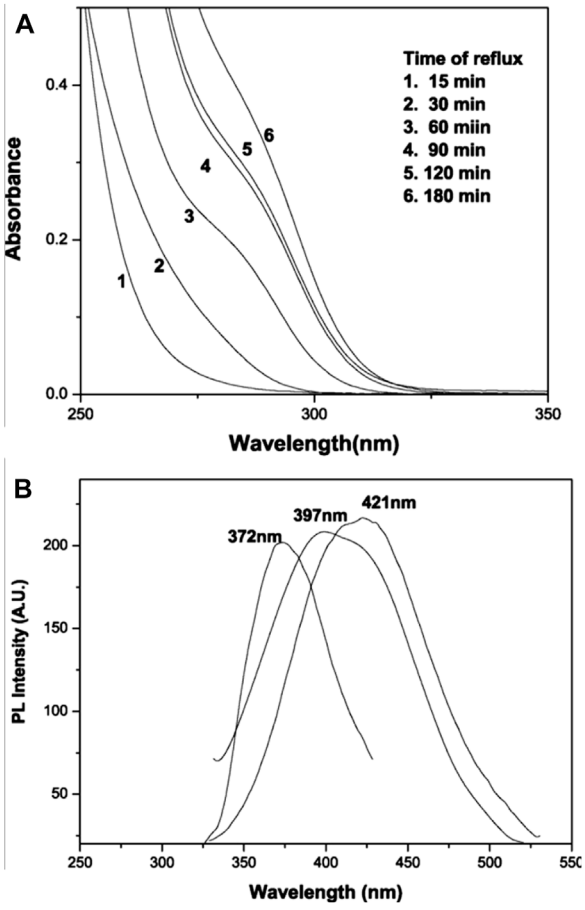


FIGURE 1
Systematic study of the growth mechanism of mercaptoethanol-capped ZnS nanoparticles with time of reflux: **(A)** absorption spectra; **(B)** photoluminescence spectra (reproduced with permission from ref 22. © 2007; Elsevier).

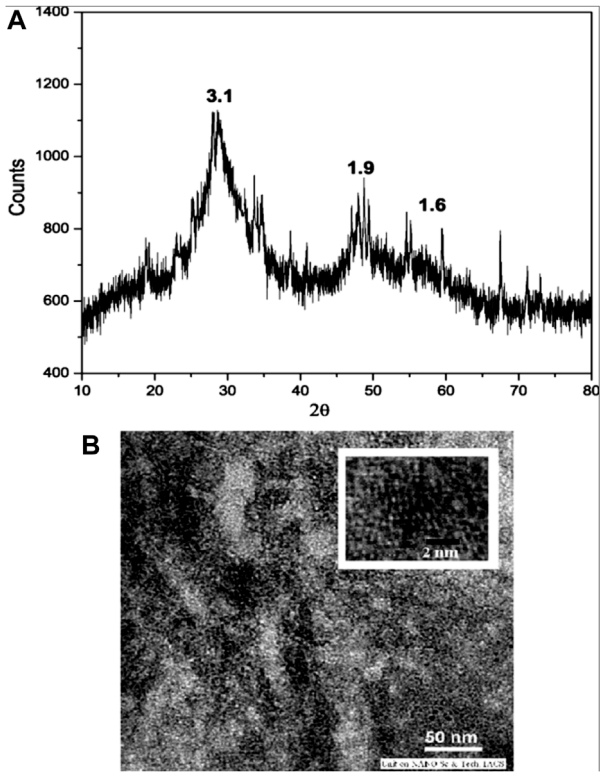


FIGURE 2
**(A)** Wide-angle X-ray diffraction pattern of cysteine-capped ZnS nanocrystals (time of reflux = 30 min); **(B)** TEM image of corresponding cysteine capped ZnS nanocrystals. Reproduced with permission from ref 22. © 2007, Elsevier).

photoluminescence. Zhai et al. (2012) used oleylamine as both solvent and capping agent to synthesize ZnS nanoparticles. This method produced highly uniform nanoparticles with tunable optical properties, making them suitable for application in light-emitting diodes (LEDs) and bioimaging. Zhao et al. (2019) developed a hydrothermal method to synthesize ZnS nanorods. By adjusting the concentration of precursors and reaction time, they achieved nanorods with high aspect ratios and excellent photocatalytic properties for the degradation of organic pollutants. Ramamoorthy and Rajendran (2018) reported a one-pot hydrothermal synthesis of ZnS hollow spheres which exhibited enhanced photocatalytic activity due to their high surface area and efficient charge separation. Yan et al. (2016) fabricated ZnS@ZnO core-shell nanostructures using two-step chemical vapor deposition. The core shell structures demonstrated better photocatalytic performance and stability than pure ZnS or ZnO nanoparticles. Hao et al. (2019) synthesized CdSe/ZnS core shell quantum dots using layer-by-layer colloidal synthesis. The ZnS shell improved the stability and quantum yield of the CdSe core, making these quantum dots highly efficient for use in display technologies and bioimaging. Advanced synthetic methodologies such as colloidal, hydrothermal, solvothermal, microwave, and core shell synthesis continue to enhance the functional properties and expand the potential applications of ZnS nanostructures in fields such as optoelectronics, photocatalysis, and biomedicine.

## 3.3 Synthesis of selenium-based zinc chalcogenides

ZnSe, a II–VI semiconductor, is widely applied in electronics and in devices such as lasers, transistors, beam expanders, and LEDs. ZnSe exhibits two primary structural forms: cubic zinc-blende (ZB) and hexagonal wurtzite (W) (Deng et al., 2007). The bandgap energy of bulk ZnSe nanocrystals is 2.7 eV (460 nm) and exciton binding energy at room temperature is 21 meV (Gudiksen et al., 2001; Wang et al., 2010). Various strategies can be employed to obtain ZnSe nanostructures (Yang et al., 2000; Zhang et al., 2004; Colli et al., 2005; Jiang et al., 2005; Fu et al., 2006; Zhai et al., 2007; Hou et al., 2010; Salem et al., 2016) including radiation, solvothermal/hydrothermal routes for nanobelts, modified vapor deposition for nanowires, metalorganic vapor-phase deposition and simple chemical vapor deposition method for nanotubes, simple thermal evaporation for nanoneedles; and low-temperature synthesis methods for nanoplates have been found.

Chestnoy et al. (1986) first synthesized ZnSe by the colloidal method, where the smallest clusters with lattice defects can be produced at −80 °C, which is a low temperature synthesis in

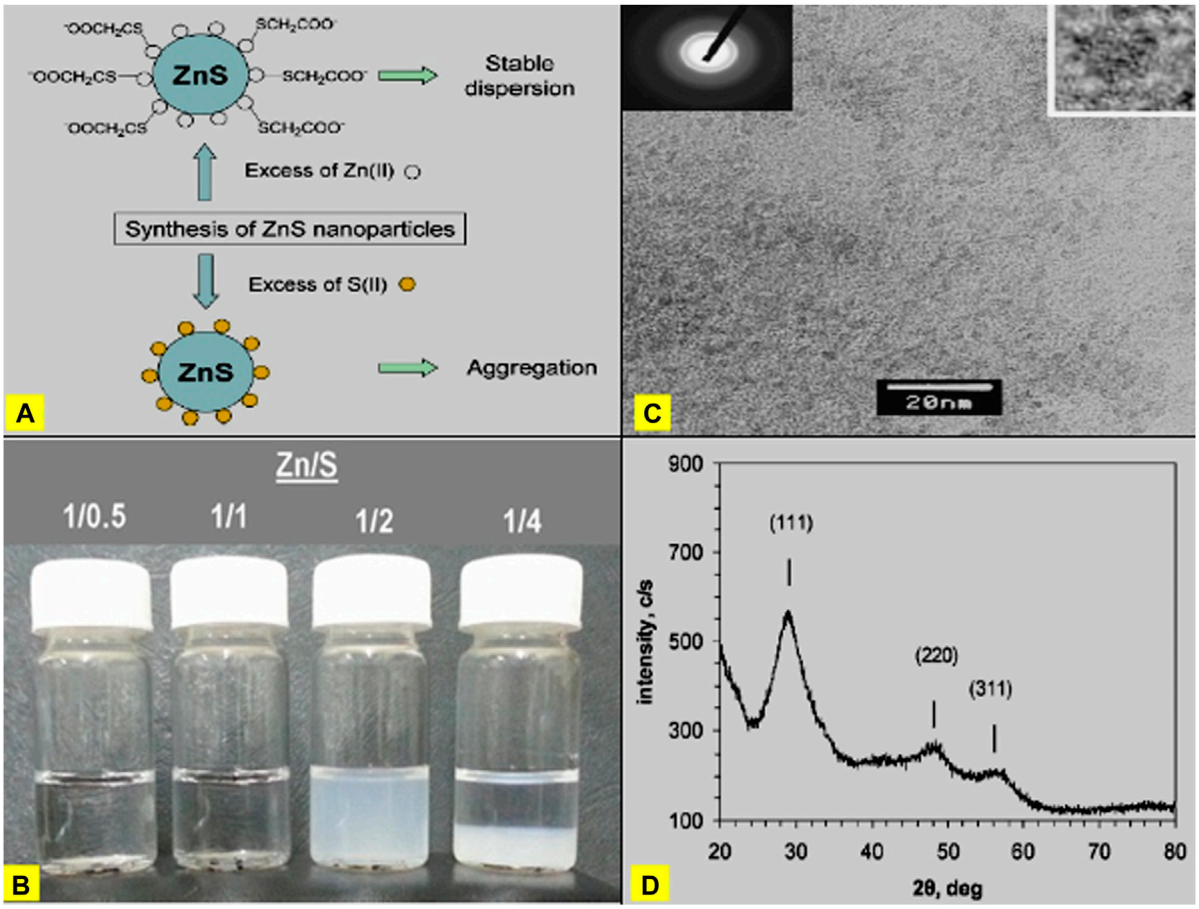


FIGURE 3
**(A)** Typical explanation of for the observed stability of ZnS nanoparticles in excess of Zn (II) precursor and observed aggregation in excess of S(II) precursor. **(B)** Images of reaction mixtures containing ZnS nanoparticles prepared at various Zn/S molar ratios (given in the legend). **(C)** TEM image of ZnS nanoparticles. Electron diffraction pattern and magnified image of a single nanoparticle are given as insets. **(D)** XRD of ZnS nanoparticles, indicating cubic (sphalerite) crystalline structure (Reproduced with permission from ref 38. © 2014; Elsevier).

2-propanol as a solvent or methanol at ambient temperature, otherwise an ethylene glycol–water mixture. They also reported a second excited electronic state of ZnSe clusters which could demonstrate the structure.

A novel organic synthesis of ZnSe quantum dots by hot injection using trioctylphosphine (TOP) as the solubilizing agent and trioctylphosphine oxide (TOPO) as the stabilizing ligand has been achieved by Azad Malik et al. (1998). In their approach, ethyl(diethyldiselenocarbamato) zinc was dissolved in TOP and injected into hot TOPO, resulting in nanocrystals that exhibited a broad band edge emission at 446 nm. The crystalline sizes of synthesized nanocrystals ranged from 3.6 to 6.3 nm.

Jun et al. (2000) presented the synthesis of ZnSe QDs in one step using air-stable complex bis(phenyl selenol)zinc–tetramethylethylenediamine (TMEDA) to grow size-dependent quantum dots based on growth temperature. In a typical synthesis, $Zn(SePh)_2$ (TMEDA) was dissolved in TOP and this reaction solution was injected into a hot TOPO solution followed by different reaction temperatures: 320 °C, 340 °C, 367 °C, or 385 °C. The ZnSe QDs obtained showed emission properties lying in the wavelength range 387–451 nm. High resolution transmission electron micrographs showed a spherical structure for ZnSe QDs with average particle sizes of 2.7–4.9 nm.

Norris et al. (2001) devised an organometallic synthesis route to prepare manganese-doped ZnSe nanocrystals using high temperature and selecting dialkyl manganese—$MnCl_2$, trioctylphosphine precursors for adopting a novel synthesis. The introduction of Mn impurity was in the limit of one per nanocrystal (or less), confirmed by EPRand magnetic circular dichroism (MCD) studies.

Karanikolos et al. (2004) presented a method for the size-dependent controlled synthesis of ZnSe nanocrystals. This involved reacting hydrogen selenide gas with diethyl zinc dissolved in heptane nanodroplets of a microemulsion. It was formed by the self-assembly of a poly(ethylene oxide)–poly(propylene oxide) amphiphilic block copolymer in formamide. By varying the initial concentration of diethyl zinc in the heptane, they were able to tune the formation of a single nanocrystal. Emission spectra analysis revealed a blue shift correlated with the average size of the ZnSe nanocrystals, determined to be approximately 6 nm.

Shavel et al. (2004) detailed the synthesis of ZnSe nanocrystals utilizing various thiol groups as stabilizing agents. This involved adding measured amounts of zinc perchlorate, thioglycerol (TG),

thioglycolic acid (TGA), and 3-mercaptopropionic acid (MPA) to a basic medium with continuous stirring. The resulting ZnSe nanocrystals exhibited stability at room temperature due to the presence of stabilizing ligands, which prevented aggregation. X-ray diffraction (XRD) studies indicated that the size of the nanoparticles were 2–3 nm and possessed a cubic structure. Additionally, the researchers observed an increase in the photoluminescence quantum yield of approximately 25%–30% after undergoing post-preparative photochemical treatment.

Qian et al. (2006) prepared ZnSe by microwave irradiation. In their approach, $ZnCl_2$, $NaBH_4$, selenium powder, and 3-mercaptopropionic acid was used as a capping agent. The size of synthesized nanocrystals was about 3.4 nm, confirmed by TEM and XRD reports suggesting that as-prepared nanocrystals belonged to a cubic structure (zinc blende). Qian et al. (2006) reported that microwave irradiation and higher reaction temperature accelerated the rapid growth of nanocrystals and also increased photoluminescence quantum yield up to 17%.

Norberg et al. (2006) investigated the preparation of $Co^{2+}$-doped ZnSe magnetic semiconductor QDs using hot injection. Their synthesis process involved zinc acetate, cobalt acetate, oleic acid, HDA (hexadecylamine), 1-octadecene, TBP (tributylphosphine), and selenium. Moreover, low-temperature electronic absorption and magnetic circular dichroism (MCD) spectra of $Co^{2+}$-doped ZnSe quantum dots revealed excitonic Zeeman splitting energies that were notably smaller than those anticipated from bulk $Co^{2+}$-doped ZnSe data. The as-prepared nanocrystals exhibited approximate spherical shapes of diameter 5 nm (Figures 4 and 5).

Experimental results, including ligand-field electronic absorption and MCD spectra, suggest a homogeneous substitutional speciation of $Co^{2+}$ in the ZnSe quantum dots. Interestingly, dopants were consistently added, keeping constant concentration at the time of growing nanocrystals, although they were absent from the central core of the quantum dots. Yang et al. (2011) utilized microemulsion to synthesize ZnSe, employing zinc acetate, sodium borohydride, selenium powder, cyclohexane, isopropanol, and Triton X-100. Their study highlighted the significant influence of the cosurfactant on regulating crystal size.

Wang et al. (2009) prepared water-soluble ZnS:Mn d-dots using mercaptopropionic acid (MPA) as the stabilizer to conduct their luminescent and photostability properties. The PL spectrum emission peak of doped nanoparticles was found at around 570 nm. The XRD data revealed a cubic zinc blende structure of synthesized nanocrystals with a diameter of 3.8 nm. The photostability of the Mn: ZnSe d-dots were measured by UV irradiation, allowing these NCs to be used for biomedical applications. Cao et al. (2010) prepared ZnSe by the solvothermal method and analyzed the photocatalytic activity of synthesized nanoparticles. PL spectra showed a broad blue emission band at 443 nm, which was attributed to the near band-edge emission and a defect-related very weak green band at 530 nm. Zhang et al. (2012) noted that CdSe/ZnSe nanocrystals exhibited a dissociation of Zn-Se in a low-temperature region, while both Cd-Se and Zn-Se dissociation occurred in a high-temperature region.

Mai et al. (2018) investigated the single-step synthesis of highly luminescent doped ZnSe:Mn nanoparticles and elucidated their interactions with acid amine. Their method involved injecting NaHSe solution into a $Zn^{2+}$ precursor solution containing zinc acetate, manganese acetate, and MPA as a capping agent. XRD spectral analysis confirmed the cubic zinc blende structure of the ZnSe nanoparticles. The interaction with acid amide led to a reduction in the number of electrons in the excited state, consequently decreasing the number of electrons transitioning from the excited state to the lowest energy level group due to the formation of an imidazole group (-CO-NH) via MPA. As a result, the addition of acid amine was found to enhance the photoluminescence intensity of the ZnSe quantum dots coated with MPA and starch, while a decrease in photoluminescence was observed in the case of MUA and PVA-coated QDs.

Assadullah et al. (2021) demonstrated the hydrothermal synthesis of ZnSe nanostructures with controlled morphologies, providing insights into the growth mechanisms and optical properties of ZnSe nanomaterials.

These diverse synthetic methodologies, ranging from colloidal to microwave-assisted approaches, underscore the versatility and tuneability of ZnSe nanostructures, promising advances in optoelectronics and material science.

## 3.4 Synthesis of tellurium-based zinc chalcogenides

Zinc telluride (ZnTe) is a noteworthy semiconductor, belonging to the P (positive)-type category; it boasts distinctive optical and electrical characteristics. Its direct bandgap of 2.26 eV (Ersching et al., 2010) at room temperature makes it a promising material for various applications. Typically, ZnTe adopts a cubic crystal structure, resembling either sphalerite or zinc blende (Promnopas et al., 2014), although it can also be synthesized in hexagonal crystals with a wurtzite structure (Dwivedi and Dubey, 2009). These structural variations significantly influence its properties. ZnTe has immense potential in solid-state devices, serving in diverse roles such as solar cells (Liu et al., 2013), photo-detectors (Shaygan et al., 2014), LEDs (Shkir et al., 2012), optoelectronic devices (Jiao et al., 2015), high-efficiency multi-junction solar cells (Löffler et al., 2005), terahertz (THz) devices (Lincheneau et al., 2014), and electronic devices (Xia et al., 2003). The efficacy of these applications relies heavily on the crystal structure and particle size of ZnTe, underscoring the importance of precise control and understanding of its material properties. ZnTe nanoparticles and quantum dots are commonly prepared with different methodologies such as thermal evaporation, microwave irradiation, chemical synthesis, electrodeposition, and spray pyrolysis (C Sharma et al., 2013; Feng et al., 2013; Kim et al., 2011; Hossain et al., 2008a).

Li et al. (1999) reported the synthesis of ZnTe nano-rods by a solvothermal process where hydrazine hydrate is taken as the solvent. Jun et al. (2001) reported the preparation of ZnTe nanocrystals through one-pot synthesis using the process called "thermolysis". They used $[Zn(TePh)_2][TMEDA]$ as a precursor. In the process of thermolysis, TMEDA dissociated to form ZnTe and $Ph_2Te$ at higher temperatures. In this typical synthesis, the zinc precursor dissolved in trioctylphosphine into the hot dodecylamine solvent at 180–240 °C over 2 hours. They found that the synthesized ZnTe nanocrystals were cubic in structure. Control of the

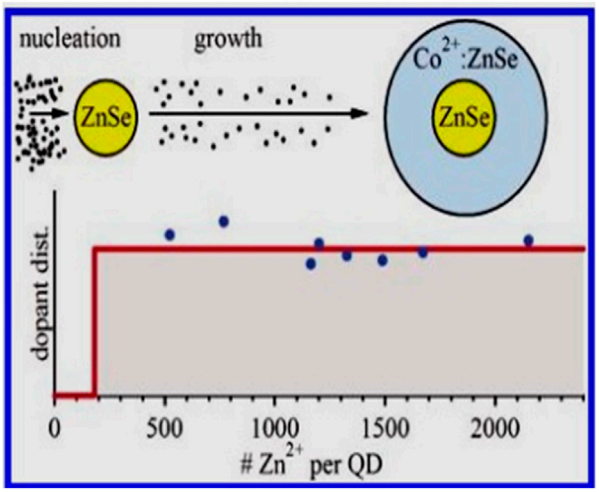


FIGURE 4
Summary of experimental dopant distribution Reprinted with permission from Norberg et al. (2006). © 2006, American Chemical Society.

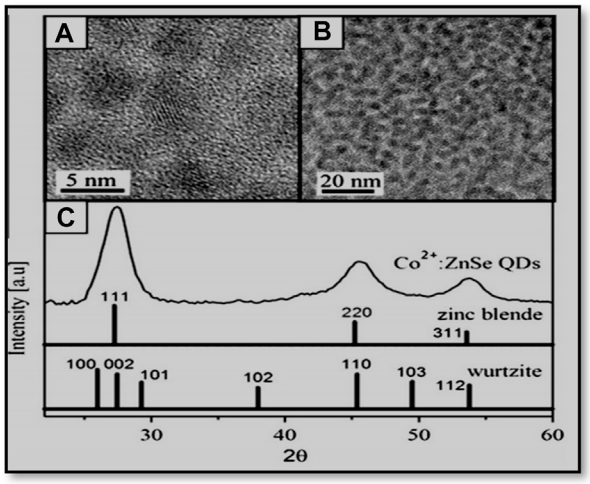


FIGURE 5
**(A, B)** TEM images and **(C)** powder X-ray diffraction of $Co^{2+}$: ZnSe QDs. Powder diffraction patterns for zinc blende and wurtzite ZnSe are included in **(C)** for comparison. Reprinted with permission from Norberg et al. (2006). © 2006 American Chemical Society.

nanocrystal size is possible by varying temperature or altering the emplaning surfactants (Figures 6 and 7).

Du et al. (2006) demonstrated the synthesis of ZnTe nanoparticles using ethylenediamine and hydrazine hydrate by the solvothermal method. They reported that synthesized ZnTe has a cubic structure. Their approach was cost-effective over the large-scale production of nanomaterials (Murray et al., 2000; Gates et al., 2002). In some cases, this process is much more effective than in those with single solvents (Yu et al., 2002).

Yong et al. (2007) prepared of ZnTe nanowires by the solution–liquid–solid (SLS) method. In this typical experiment, they injected (TOP)Te solution into a mixture of zinc oxide, phenyl ether, myristic acid, and hexadecylamine, which was heated to 250 °C. The resultant ZnTe nanocrystals were precipitated by the addition of chloroform with a cubic structure. They seem to have formulated a new method following a new multiple nucleation growth model which aids the understanding of the growth mechanism of nanowires.

Ghosh et al. (2011) proposed a simple strategy for synthesizing stable, fluorescent ZnTe/dendrimer nanocomposites via an aqueous route with the variation of dendrimer terminal groups. In this approach, a solution of NaHTe was swiftly injected into a dendrimer solution containing $Zn^{2+}$ ions. NaHTe solution was prepared using telluric acid dissolved in water, and the solution was heated with sodium borohydride with continuous nitrogen flow. There were varying terminal groups of dendrimers and observed size tunability in synthesized ZnTe ranging from 2.9–6.0 nm with a photoluminescence quantum yield of almost 15%. Jiang et al. (2010) reported a hot injection synthesis procedure of ZnTe QDs. A novel ligand tuning method was used to assemble nanocrystals which can tune their size and morphology and also assemble them into more complex architectures. They used pure oleylamine as a solvent, Zn $(Et)_2$ as a zinc precursor, and TOPTe as a tellurium precursor.

Zhang et al. (2011) discovered by hot injection that they could produce ZnTe by hot injection using two precursors of tellurium (Te) metal: tellurium-trioctylphosphine and polytellurides. They injected freshly prepared Te precursor solution into a zinc solution. The temperature of the system was increased 190–300 °C after the nucleation stage, producing ZnTe nanocrystals. A trial experiment was conducted by injecting a tellurium source solution at 250 °C, yielding ZnTe (ZB phase). They observed that the nanocrystals formed were in the WZ instead of ZB phase as the mixture was heated to 300 °C.

Dantas et al. (2012) proposed the synthesis of $Mn^{2+}$-doped ZnTe nanoparticles on glass as host matrix named as a fusion method. They synthesized ZnTe nanoparticles using two sequential melting–nucleation approaches using a PZABP glass matrix and a concentration ratio of Mn as a dopant and Zn-precursor concentration, resulting in the growth of $Zn_{1\_x}MnxTe$ NCs by thermal annealing in the glass template. Cubic zinc blende structures were developed in glass matrices to grow nanoparticles of ZnTe. The structure did not alter by doping ZnTe nanoparticles with $Mn^{2+}$ ions.

Mntungwa et al. (2012) used $ZnCl_2$ and NaHTe as precursor molecules and HAD as a capping agent to synthesize ZnTe nanoparticles. NaHTe was prepared by using tellurium powder, which was mixed with deionized water and a reducing agent of sodium borohydride under $N_2$ atmosphere. Aqueous solution of $ZnCl_2$ was added to the above solution, stirred, and dispersed in tri-n-octylphosphine to obtain a TOP–ZnTe solution. This was injected at 230 °C or 270 °C into a hot HDA solution. The XRD result shows that a cubic zinc-blende structure of ZnTe, similarly cubic, and water soluble ZnTe nanowires was formed by ligand exchange (Deng et al., 2013).

Hou et al. (2013) synthesized a single crystalline and highly fluorescent single-ZnTe nanorod via a liquid–liquid interface reaction of zinc acrylate with NaHTe using oleic acid as a capping ligand under 90 °C. This helped to achieve diverse nanoparticle structures via the efficient fabrication of

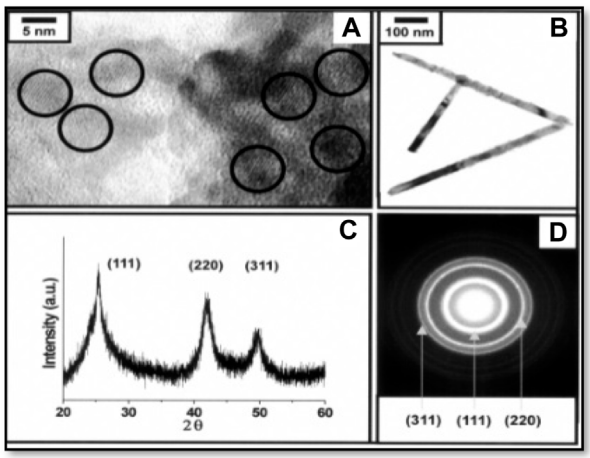


FIGURE 6
**(A)** HRTEM image analysis of ZnTe quantum dots showing spherical shape grown at 240 °C **(B)** TEM image of rod-like ZnTe nanocrystals **(C)** XRD pattern **(D)** SAED (selected area diffraction patterns) of 4.2 nm ZnTe quantum dots. Reproduced with permission from ref 101. © 2001, Royal Society of Chemistry.

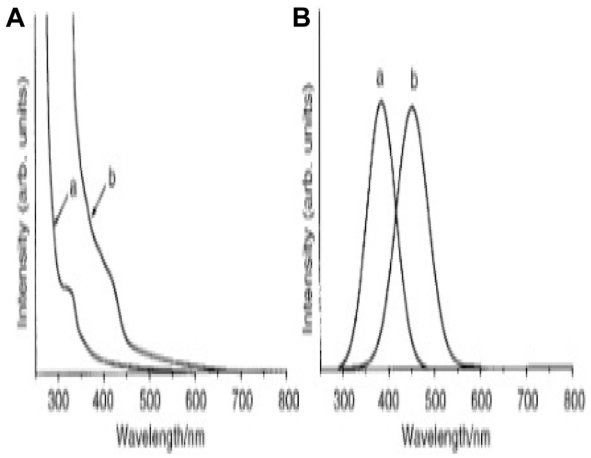


FIGURE 7
Absorption spectra of zinc telluride quantum dots grown at **(A)** 240 and **(B)** 180 C**(A)** UV–VIS absorption spectra, **(B)** Photoluminescence spectra (Reproduced with permission from ref 101. © 2001, Royal Society of Chemistry.

nanoparticles. They noted that as the temperature increased over 100 °C, the PL intensity decreased, which might result in the detachment of the excessive ligands from the surface of nanoparticles. The fluorescence quantum yield was 60% as observed in blue region. This approach was similar to the synthesis of water-soluble cysteine-capped zinc telluride at the low temperature route by Dunpall et al. (2014) that involved injecting NaHTe solution into the mixture of $ZnCl_2$ and L-cysteine ethyl ester hydrochloride (capping agent). They observed the transition of nanospheres of 40–50 nm into nanorods with a size range 60–80 nm long and 20–25 nm in diameter.

Dhungana et al. (2016) reported the aqueous synthesis of ZnTe at room temperature and pressure—a chemical precipitation technique. In their approach, zinc telluride nanoparticles were prepared with a 1:1 M ratio of $Zn^{2+}$:$Te^{2-}$ using $Zn^{2+}$ and NaHTe at 90 °C. Their ZnSe nanocrystals possessed cubic structures influenced by the source compound of zinc as well as the dilution of the size and structure of the ZnTe nanocrystallines (Figure 8).

Interestingly, Luo et al. (2017) synthesized the vertically aligned core shell heterostructure of ZnO/ZnTe core/shell nanocrystals and applied them in photovoltaic devices. Alternatively, Sadaqat et al. (2019) found that they could produce ZnTe nanospheres via a hydrothermal method. They added hydrazine monohydrate to a solution of $ZnCl_2$, tellurium powder, and KOH. They placed the mixture in a Teflon-lined stainless autoclave for 3 h at 200 °C. The resultant ZnTe nanospheres formed were cubic in structure. They demonstrated water splitting catalysis by synthesized ZnTe nanospheres which act as electro-catalysts.

Recent advances have been made in the synthesis of ZnTe nanostructures, further expanding the toolkit of synthetic methodologies. For instance, Ilanchezhiyan et al. (2018) demonstrated the sonochemical synthesis of ZnTe nanostructures with controlled morphologies, providing insights into the photoelectronic functionalities of ZnTe nanomaterials. These diverse synthetic methodologies, including hydrothermal, solvothermal, thermolysis, and fusion methods, provide a comprehensive toolbox for tailoring the properties of ZnTe nanostructures to meet the demands of various applications.

In general, various synthesis methods have been employed for the fabrication of Zn chalcogenide nanomaterials, each offering distinct advantages. Colloidal synthesis involves the reduction of precursor ions in a liquid phase, yielding highly uniform nanoparticles with precise control over size and shape using a surface capping agent. This method is scalable and allows the production of large quantities of nanomaterials suitable for industrial applications. On the other hand, hydrothermal synthesis operates in an aqueous environment under elevated temperatures and pressures, promoting the growth of high-quality crystalline materials with enhanced control over morphology and phase purity. The use of water as a solvent makes hydrothermal synthesis environmentally friendly. Solvothermal synthesis is similar to hydrothermal synthesis but employs organic solvents, enabling higher reaction temperatures and the synthesis of materials with low solubility in water. Solvothermal methods offer tailored properties and are suitable for complex nanostructures. Microwave-assisted synthesis stands out for its rapid reaction times and uniform heating, leading to shorter synthesis durations and energy-efficient processes. This method is ideal for high throughput production and offers control over particle size and distribution. Additionally, core-shell synthesis involves coating core materials with a shell of another material, enhancing properties and functionalities while protecting the core from degradation. Core-shell structures are highly customizable and are applied in catalysis, sensors, and biomedicine. In summary, the choice of synthesis method depends on factors such as desired properties, scalability, reaction speed, environmental considerations, and the complexity of the nanostructures required for specific applications in Zn chalcogenide research and development.

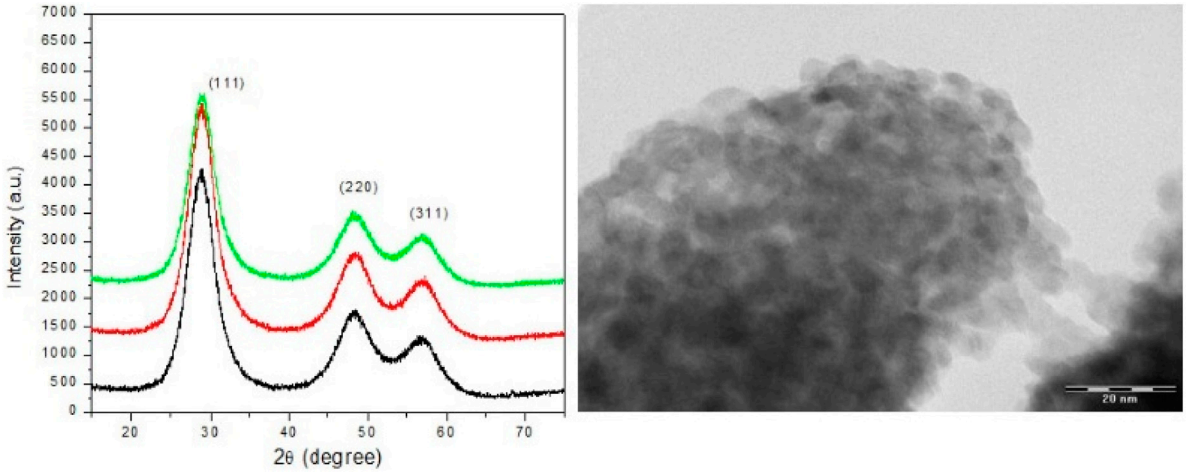


FIGURE 8
X-ray diffraction pattern of zinc telluride nanocrystals by aqueous synthesis with variation of molar ratio ($Zn^{2+}$:$Te^{2-}$) by various dilutions along with TEM image of ZnTe nanocrystals, (Reproduced with permission from ref 117. © 2016; Nepal Academy of Science and Technology).

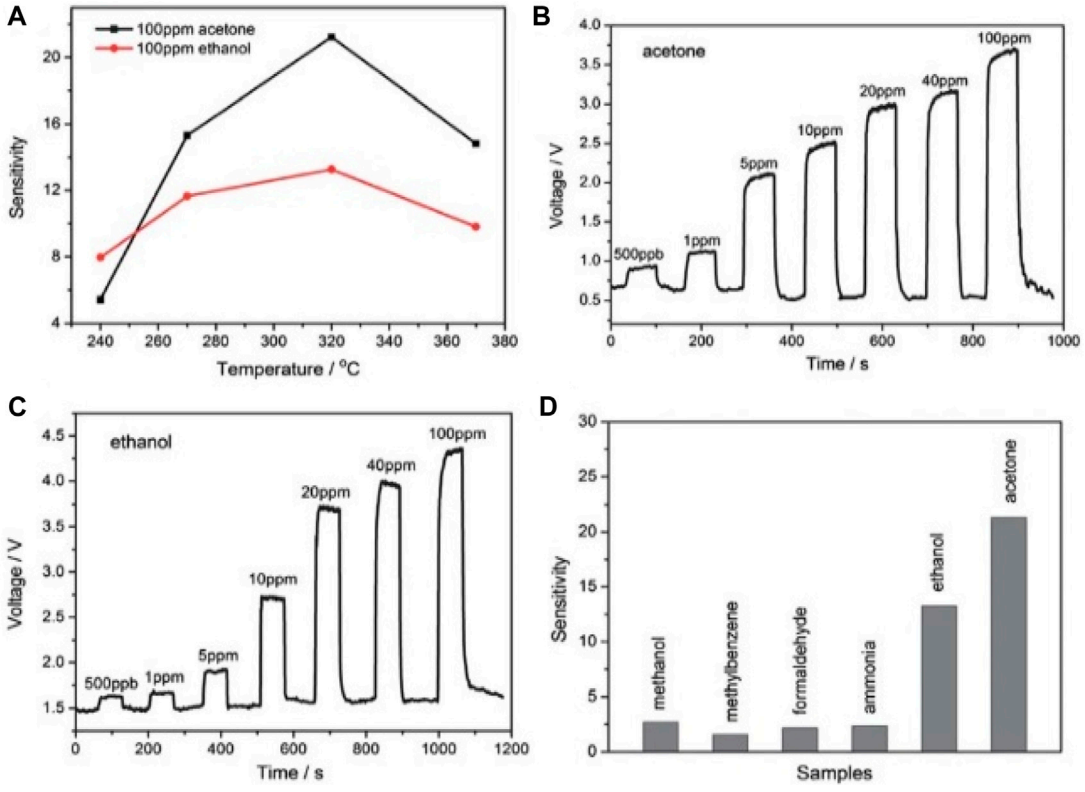


FIGURE 9
**(A)** Investigation of sensitivity of ZnS nanowire gas sensors: sensor sensitivity vs. operating temperature of the synthesized dynamic response–recovery curves of the gas sensor towards volatile organic compounds at a series of concentrations: **(B)** acetone; **(C)** ethanol. **(D)** Sensing response of gas sensors to different gases with a concentration of 100 ppm (Reproduced with permission from ref 121. © 2012; Royal Society of Chemistry).

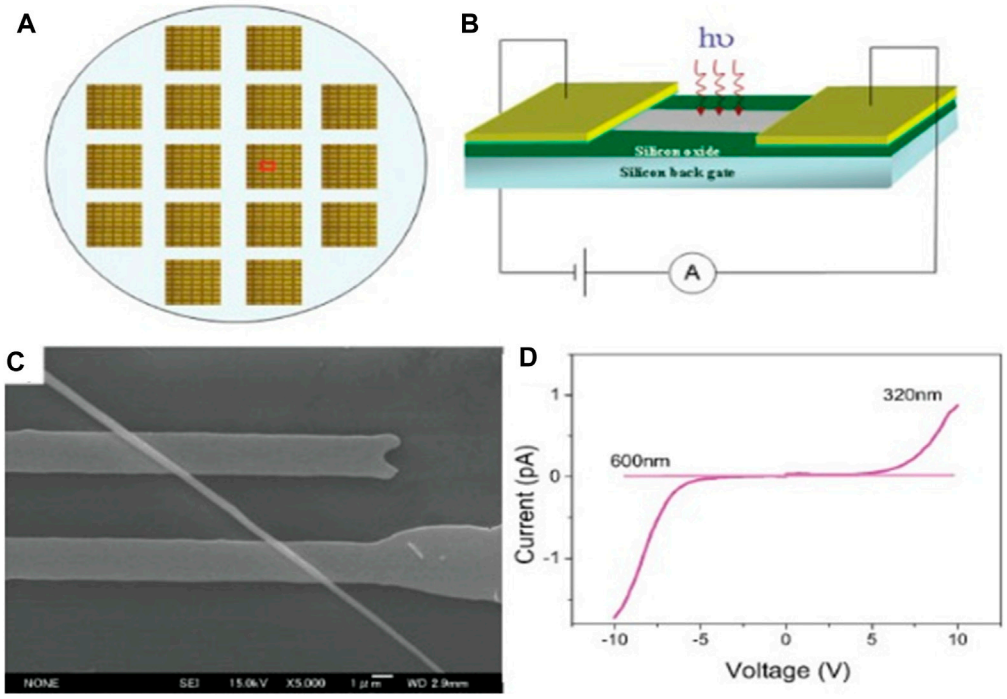


FIGURE 10
**(A)** Optical microscopy image of individual ZnS-nanobelt-based UV-light sensor array composed of individual structures. **(B)** Schematic diagram of individual ZnS-nanobelt-based UV-light sensor configuration. **(C)** SEM image of single-crystalline ZnS-nanobelt device taken from marked area in **(A)**. **(D)** I–V characteristics of individual ZnS-nanobelt-based UV-light sensor illuminated with different wavelengths of 320–600 nm (Reproduced with permission from ref 122. © 2009; Wiley).

# 4 Applications of different Zn chalcogenides

## 4.1 Sensors

Zinc sulfide (ZnS) has emerged as a promising material for sensing due to its different morphology and wide bandgap. Wang et al. (2012) successfully crafted nanowire-based gas sensors and UV light-sensor thermistors by utilizing nanowires as the active component. ZnS exhibits high sensitivity and rapid response to UV light, indicating its significant potential for UV-light photodetectors. This potential stems from ZnS nanowires' wide bandgap of 3.77 eV, a crucial characteristic (Figure 9). Additionally, Wang et al. (2012) revealed the thermosensitivity of ZnS nanowires, demonstrating a substantial current enhancement from 1.65 × 10-7A to 1.89 × 10-4A—a remarkable 1000-fold increase.

Fang et al., 2009 detailed the fabrication of UV-light photodetectors based on ZnS nanobelts. Their findings reveal that the photo response of an individual ZnS nanobelt-based UV-sensor increases more than thrice in magnitude when illuminated with 320 nm light irradiation compared to its response to visible light. This heightened sensitivity to UV light, coupled with high spectral selectivity, positions ZnS as a promising UV detector in this specific wavelength range. These attributes are clearly depicted in Figure 10.

$Mn^{+2}$-doped ZnS QDs have been used to sense the explosive compound 2,4,6-trnitrotoluene (TNT) by photoluminescence. A quenching study of earlier pure ZnS QDs has also been used for the decomposition of organic dyes through photocatalytic degradation. Among other applications, Naeimi et al. (2014) synthesized unsubstituted-1,5-benzodiazepine using ZnS nanoparticles as new catalyst useful for fuel cells in ethanol production.

Future research directions in this field could focus on further enhancing the sensitivity, selectivity, and stability of zinc-chalcogenides-based sensors. Additionally, advances in material synthesis techniques, such as precise control over morphology and surface properties, can lead to improved sensor performance and enable the development of novel sensing applications. Continuing research efforts are crucial for unlocking the full potential of zinc chalcogenides in sensor technology and addressing emerging challenges in sensing various environmental and biological parameters.

## 4.2 Biomedical imaging

Bioimaging is one of the best tools for disease diagnosis and the treatment of cancer cells by labeling with highly fluorescent nanoparticles and core shell quantum dots. Charvet et al. (2004) conducted bio imaging experiments that utilized biotinylated CdSe/ZnSe core-shell nanocrystals in an aqueous environment to demonstrate their suitability for fluorescent biological imaging. Their method involved fixing neuronal cells from mouse embryo cerebellum grown on polylysine glass covers for 5 days with 4% paraformaldehyde solution. Subsequently, the cells were

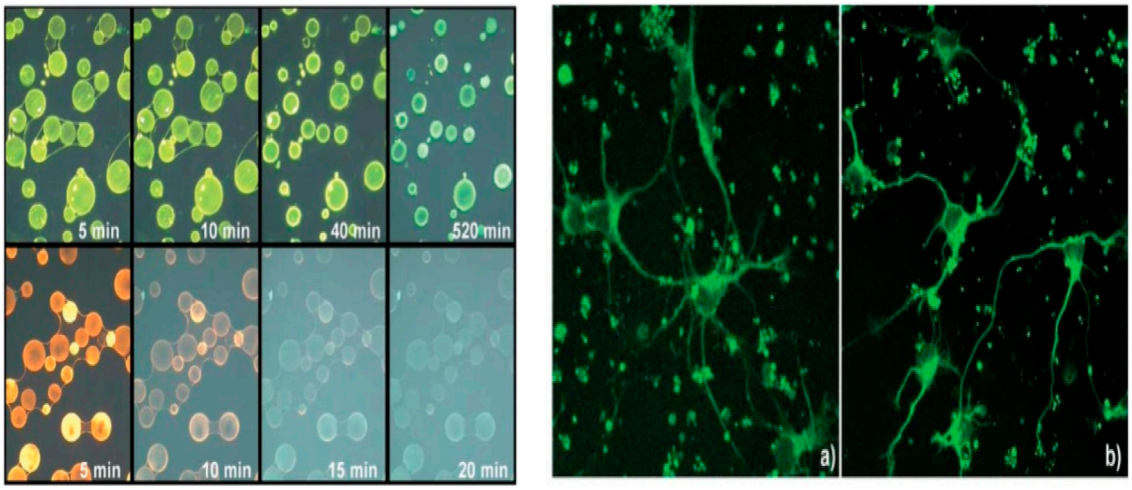


FIGURE 11
**(A)** Fluorescence images of agarose beads labeled with biotinylated nanocrystals (top row) and biotinylated R-Phycoerythrin (bottom row). Mean size of beads is 50 mm. Under continuous irradiation with a mercury lamp (100 W), photos are taken at different time intervals using an Olympus Microscope equipped with a U-MWU band pass filter (cut-off 330–385 nm). **(B)** Fluorescence image of nerve cells in primary culture labeled with biotinylated nanocrystals (excitation wavelength 458 nm). Control experiment done with Alexa-488 labeled. Reproduced with permission from ref 124 © 2004, Royal Society of Chemistry (Charvet et al., 2004).

permeabilized using Triton X100. Then, an antigen–antibody binding technique was implemented to level the damaged cell with fluorescent nanocrystal. The neuronalmicrotubule-specific primary antibody TuJ1 was applied, followed by a biotinylated secondary antibody and streptavidin incubation, leading to the binding of biotinylated nanocrystals. This method facilitated the fluorescent labeling of nanocrystals which targeted specific nerve cells where TuJ1 antibodies were located, showcasing their potential for intracellular labeling (Figure 11).

Similarly, Saikia et al. (2013a;2013b) synthesized a specific compound by making an alloy complex of the metals Zn, S, and Se for bioimaging. They conducted a comparative cytotoxicity assessment on mammalian lymphocytes for both ZnSe(S)-alloyed nanocrystals and pure zinc selenide quantum dots. Their findings revealed that the alloyed system maintained the high biocompatibility characteristic of ZnSe systems compared to the pure zinc selenides. Additionally, *in vitro* assays demonstrated a synergistic photoluminescence enhancement in the alloyed system.

Selvaraj et al. (2017) reported the creation of $Mn^{2+}$ ion-doped ZnSe (core)/ZnS (shell) nanorods using a heating method for the core synthesis followed by a hot injection technique for the shell. They observed a positive red shift in photoluminescence, achieving a quantum yield of 49.35%. These nanorods exhibited excellent permeability in human HEK293 and HeLa cells, making them suitable for bioimaging. The study highlighted a clear relationship between quantum yield, lifetime, $Mn^{2+}$ content, and ZnS shell thickness.

In a separate study, Singhal et al. (2019) used glutathione (GLT)-functionalized Mn-doped ZnS quantum dots (QDs) as fluorescent materials for bioimaging. The GLT capping rendered the ZnS QDs stable and minimized autofluorescence, with a tuned bandgap allowing activity in the 650–950 nm wavelength range. Additionally, a microfluidic approach was used to synthesize monodispersed ZnS nanoparticles doped with various luminescent ions ($Mn^{2+}$, $Eu^{3+}$, $Sm^{3+}$, $Nd^{3+}$, and $Yb^{3+}$). These nanoparticles demonstrated strong luminescence properties and reduced self-quenching, making them highly suitable for optical bioimaging applications.

Further research in the bioimaging application of zinc chalcogenides would focus on improving biocompatibility, enhancing imaging resolution and sensitivity, exploring multifunctional capabilities (such as theranostics), and developing novel synthesis methods for more complex nanostructures. Recent advances in nanotechnology, materials science, and bioconjugation techniques offer exciting possibilities for advancing zinc chalcogenides as versatile and effective bioimaging agents.

## 4.3 Photocatalytic application

A photocatalyst is defined as a substance that accelerates a chemical transformation under light exposure in the presence of a catalyst that absorbs light and participates in the reaction. Semiconductors like ZnSe are utilized as efficient photodiodes; as thin film in silicon solar cell applications (Cheng et al., 2013), they have been also utilized as photocatalysts due to their ability to address environmental challenges (Yang et al., 2012) such as water and air related contaminants. Xiong et al. (2007) reported that zinc selenide possessing a nanobelt morphology exhibited better photodecomposition efficiency than zinc selenide under equivalent UV light exposure conditions. Their experiment focused on monitoring the adsorption and photocatalytic degradation process of fuchsine acid in the presence of a catalyst. This was accomplished by the absorption of fuchsine acid at 545 nm. The aqueous solution of fuchsine acid was examined when irradiated under ultraviolet light exposure along with ZnSe nanoparticles for different durations, and absorption were measured by UV-visible spectroscopy. This experiment evidenced a significant reduction in the intensity of dye over time. Eventually,

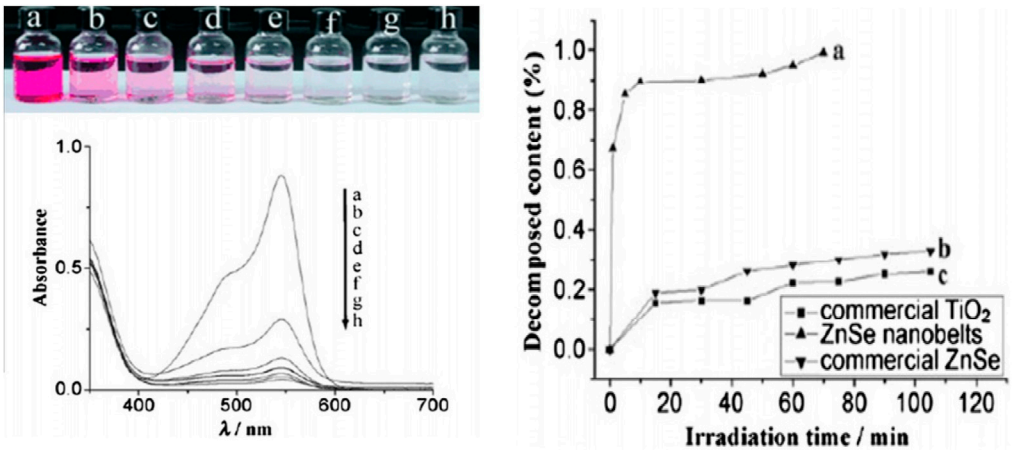


FIGURE 12
**(A)** Color change and absorption spectrum of a solution of fuchsine acid (1.0"104 m, 20 mL) in the presence of ZnSe nanobelts (10 mg) under exposure to UV light: **(A)** initial solution; **(B–H)** solutions with addition of ZnSe nanobelts, illuminated for **(B)**1, **(C)** 5, **(D)** 10, **(E)** 30, **(F)**50, **(G)** 60, and **(H)** 70 min (top and middle). **(B)** Fraction of degraded fuchsine acid in the presence of ZnSe nanobelts, commercial ZnSe, and commercial $TiO_2$ powders, as photocatalysts under exposure to UV light (bottom) (Reproduced with permission from ref 131. © 2011, Wiley.

the absorption completely vanished compared to the initial intensity of fuchsine acid (Figure 12).

Chen et al. (2012) investigated efficiency in photocatalysis by nitrogen-doped graphene/ZnSe; they described low temperature one-pot hydrothermal synthesis for the nanocomposite GN-ZnSe. This composite displayed remarkable photocatalytic efficacy due to electron hole recombination. Their findings indicated that the synthesized nanocomposites exhibited enhanced electrochemical properties for reduction reactions of $O_2$ and the photocatalytic fading of methyl orange dye under visible-light exposure.

Zhou and Zhuang investigated the photocatalytic potential of two-dimensional tetragonal (t-) ZnX (X = S, Se) with modeled layered structures, identifying a tunable bandgap that makes these materials promising for energy storage and conversion (Zhou et al., 2017). Fundamental information on the electronic structure, optical properties, and stability of various t-ZnX (X = S, Se) layered structures was derived from DFT calculations, phonon calculations, and molecular dynamics simulations. Liu et al. (2021) developed a $Cd_{0.5}Zn_{0.5}S$ (CZS) nanotwin photocatalyst by creating a twin boundary homojunction on the catalyst surface through a two-electron Z-scheme mechanism, demonstrating high efficiency in producing $H_2$ and $H_2O_2$ from water splitting under visible light irradiation. Recently, a low temperature synthesis of ($ZnIn_2S_4$) microspheres has been performed by Imran et al. (2022) for the photocatalytic degradation of malachite green, methyl orange, and direct red 80 dyes. They found that a microporous structure is more suitable for the degradation of cationic pigments than anionic pigments with high photodegradation efficiency. A mechanism of the photocatalytic degradation is given in Scheme 2 below, indicating $ZnIn_2S_4$ as a potential candidate for dye degradation.

Zinc chalcogenide photocatalysis may include future exploration of novel composite materials, understanding and optimizing charge carrier dynamics, enhancing visible-light absorption, improving the stability and recyclability of catalysts, and up-scaling production for practical applications. Recent advances in materials synthesis, computational modeling, and characterization techniques offer exciting opportunities for further enhancing the photocatalytic performance of zinc chalcogenides.

## 4.4 Light emitting phosphors application

Shao et al. (2011) developed doped nanocrystals of ZnSe quantum dots. These nanocrystals—specifically Mn-doped ZnSe (Mn:ZnSe d-dots) —were prepared in water solution and demonstrated potential as single white-light generating phosphors for solid-state light. The emission of white light from these nanocrystals is attributed to the combined emission originating from non-coordinated surface selenium sites and yellow light emitting $Mn^{+2}$ ions.

Ashwini et al. (2020) synthesized zinc sulfide doped with samarium ions by co-precipitation and performed structural, optical, and photoluminescence analyses. Their studies confirmed the successful doping of $Sm^{3+}$ without affecting the crystal structure, and photoluminescence spectra revealed two emission peaks in the orange region (603 nm) and one in the red (701 nm) due to f–f transitions of $Sm^{3+}$ in the $4f^5$ configuration. Tuan et al. (2021) discussed the emission properties of $Ce^{3+}$ and $Eu^{3+}$ ions doped ZnS. After detailed characterization, photoluminescence results showed the emission characteristics of the 3+ state electronic energy, with CIE coordinates indicating that ZnS: $Ce^{3+}$ and ZnS: $Eu^{3+}$ are suitable for optical display applications. Omata et al. (2019) fabricated $Zn(Te_{1-x}S_x)$ quantum dots (QDs) with a ZnS shell using the standard hot-injection method. These QDs exhibited photoluminescence across the visible spectrum, with a narrow band in the blue region and a broad band from green to red emissions due to exciton recombination. The alloyed form demonstrated a lower (Figure 13).

Future research in zinc chalcogenides for light-emitting phosphor applications may include exploring novel dopants and synthesis methods to enhance luminescence efficiency, tuning emission spectra for specific applications, improving stability and

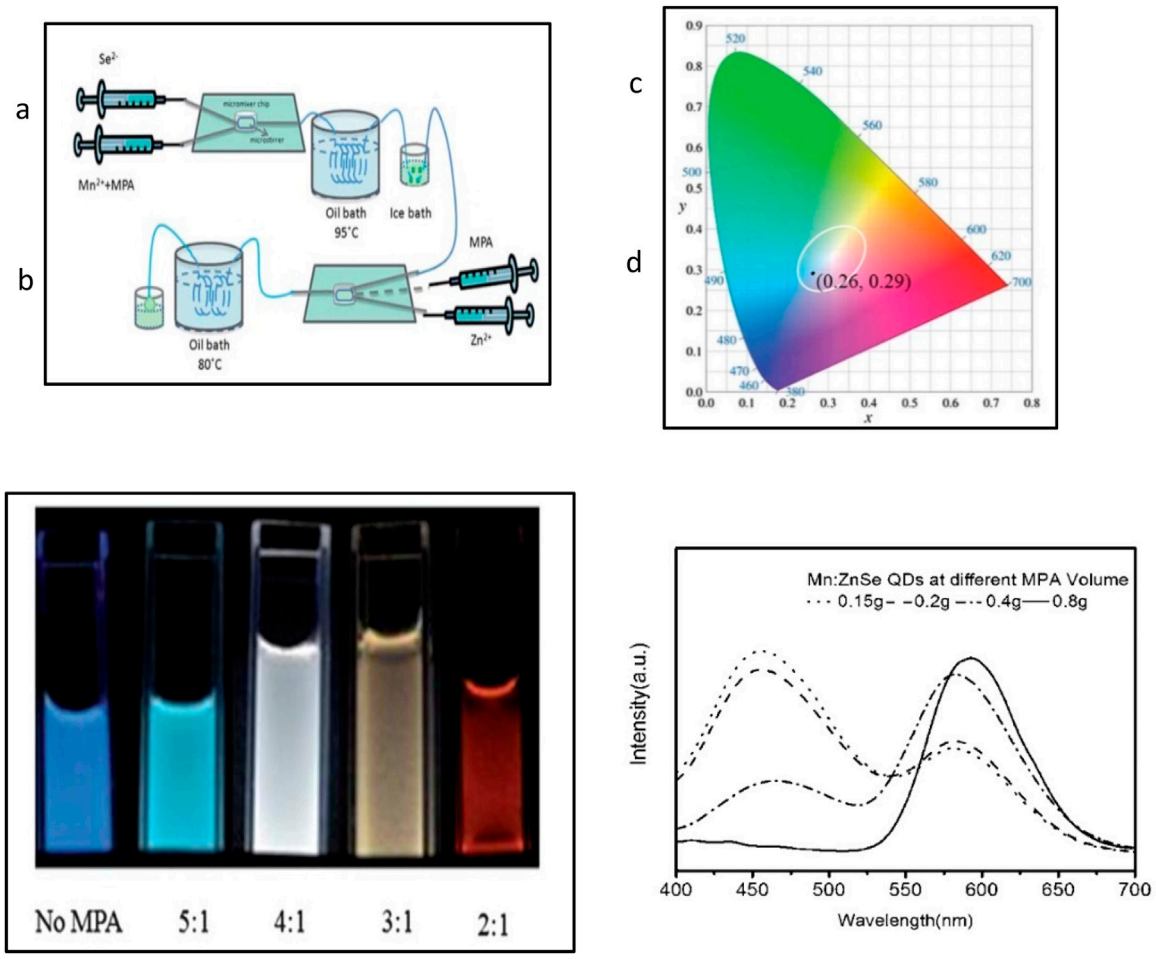


FIGURE 13
**(A)** Synthesis schematics of white-light emission $Mn^{2+}$-doped ZnSe QDs. **(B)** Digital pictures of d-dots at different [Zn]/[Mn] flow volume ratios. **(C)** Chromaticity picture of $Mn^{2+}$–doped ZnSe with white light. **(D)** PL spectra corresponding to **(B)** (Reproduced with permission from ref 136. © 2001, Royal Society of Chemistry.

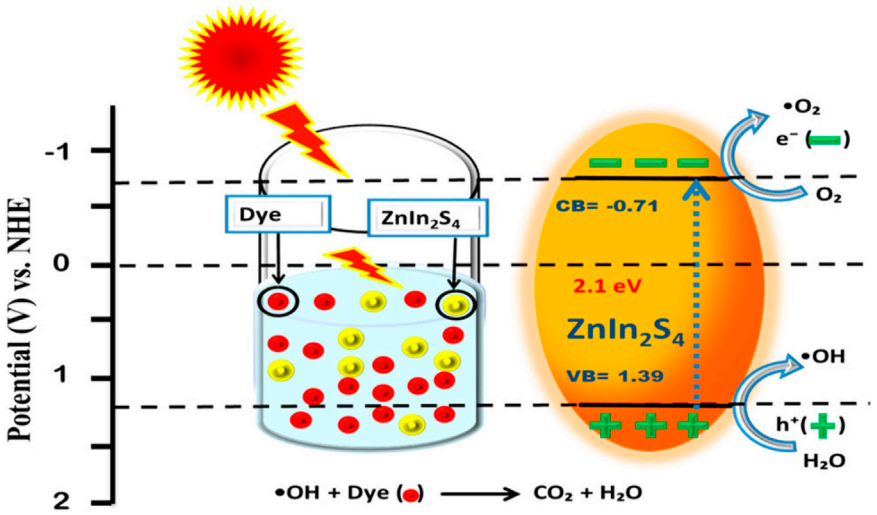


SCHEME 2
Schematic representation of the mechanism for understanding photocatalytic decomposition of dyes by $ZnIn_2S_4$ microspheres (Imran et al., 2022).

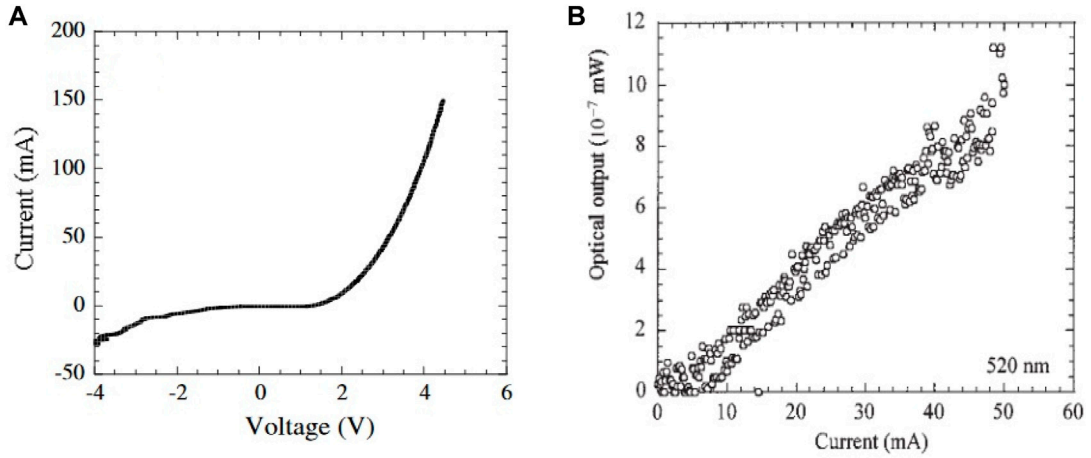


FIGURE 14
**(A)** Current–voltage characteristic of the LED structure. Measurements performed at room temperature. **(B)** Current–light output characteristic of the LED structure. The detected wavelength is 520 nm (Reproduced with permission from ref 141. © 2002, Wiley.

durability, and integrating these materials into practical devices for lighting, displays, and optoelectronic applications. Recent advancements in materials synthesis, characterization techniques, and device integration offer exciting prospects for further advancing zinc chalcogenides in light-emitting phosphor applications.

## 4.5 Optoelectronic applications of chalcogenide nanostructures

For a considerable time, ZnTe nanocrystals have been under scrutiny for their highly photoluminescent properties, particularly in optoelectronic applications. Hieu et al. (2020) investigated the composite structure of ZnTe-ZnO, which exhibited superior sensing capabilities characterized by excellent repeatability, stability, linearity, and gas selectivity, especially at temperatures exceeding 200 °C.

In their investigation, $H_2S$ gas sensing was done in the presence of ZnTe and ZnO nanorods, which notably enhanced sensing performance. They observed that a thin coating of ZnTe played a crucial role in enhancing the response characteristics of nano-transducer. The introduction of a thin ZnTe layer facilitated control over the resistance of the ZnO nanorod sensor through p–n junction formation. This contribution led to an amplified sensing response without compromising sensing kinetics. Furthermore, the study examined how p–n junction formation could serve as an effective strategy for enhancing sensor performance by modulating sensor conductance.

Hossain et al. (2008b) emphasized the promising potential of ZnTe boasting a bandgap of 2.20–2.26 eV for utilization in photovoltaic and photoelectrochemical cells. Its cost-effectiveness coupled with a high absorption coefficient renders it a compelling candidate for such device applications (Figure 14).

Ueta and Hommel (2002) showcased the fabrication of pure-green and green–yellow LEDs and the effectiveness of using ZnTe thin films and Zn-rich alloy-like ZnCdTe films in the LEDs within the wavelength range of 505–560 nm. ZnTe's bandgap energy lies in the green wavelength region at room temperature, making it well-suited for these applications. Additionally, the integration of ZnTe-based material systems, which exhibit lattice matching with ZnTe substrates such as ZnMgSeTe and ZnCdSeTe, has been proposed for the advancement of light-emitting devices with high-performance in future devices (Chang et al., 2002; Yoshino et al., 2002; Hussain et al., 2018).

Moreover, ZnTe finds its niche in heterojunction solar cells, especially when combined with CdTe. Heterojunction solar cells incorporating CdTe/ZnTe/CdS configurations have demonstrated commendable efficiency (Späth et al., 2005) (Figure 14). This multifaceted utility of ZnTe across various optoelectronic and photovoltaic domains underscores its pivotal role in advancing renewable energy technologies (Gessert et al., 1995; Feng et al., 1996).

To sum up, zinc chalcogenide nanostructures exhibit immense potential across various applications but face certain drawbacks that hinder their optimal performance. These limitations include susceptibility to oxidation or degradation, challenges in controlling morphology and size distribution, issues with agglomeration and dispersion, and concerns about toxicity, especially in cadmium-containing chalcogenides. Several strategies can be employed to overcome these challenges. Surface functionalization can enhance stability and dispersibility while mitigating toxicity concerns, making the nanostructures more compatible with biological systems. Advanced synthesis techniques like atomic layer deposition (ALD) and molecular beam epitaxy (MBE) offer precise control over morphology and composition, leading to uniform and tailored nanostructures with improved properties. Designing core shell structures and employing doping or alloying can further enhance stability, functionality, and safety. Encapsulation within protective matrices or composites also improves stability and compatibility. By leveraging these strategies, zinc chalcogenide nanostructures can be optimized for diverse applications while addressing their inherent limitations, paving the way for further technological advances. The overall synthesis methods and diverse applications of Zinc chalcogenides are detailed in Table 1.

TABLE 1 Synthesis properties and applications of zn-chalcogenides.

| Material | Size and morphology | Reactants | Method and Temperature | Applications | References |
|---|---|---|---|---|---|
| Mercaptopropionic acid capped ZnSe | Quantum dots cubic crystal structure with diameter range 4–5 nm | Zn $(OAc)_2$, $2H_2O$, $NaBH_4$, MPA, selenium powder | Colloidal synthesis, Reflux at 100°C | Photoluminescence 400–700 nm | Chatterjee et al. (2021) |
| Pristine -ZnSe nanoparticles | Quantum dots 4 nm, single cubic phase | Elemental selenium, $ZnCl_2$ | Hydrothermal | Room temperature photoluminescence | Assadullah et al. (2021) |
| ZnSe microspheres | Nanoparticles | Selenophene ($C_4H_4$ Se) and $ZnCl_2$ | Solvothermal | Photocatalytic degradation of MO dye under UV and visible light | Cao et al. (2010) |
| Mn-doped ZnSe D-Dots | Quantum dots, Mn:ZnSe d-dots 3.8 nm | $Se^2$ and $Mn^{2+}$ solutions separately encased in glass syringes and then injected into a blender using syringe pumps. | Microfluidic reactor synthesis | Mn:ZnSe d-dots emit white light with a quantum yield of about 10.2% | Shao et al. (2011) |
| Thiol-capped ZnS nanoparticles | Quantum dots | Flavin, GOD | Colloid chemical, reflux at 100 °C | Sensing of enzymes by fluorimetric quenching | Chatterjee et al. (2012) |
| Starch capped ZnS | Nanosize 2–8 nm | $ZnCl_2$, $Na_2S$, and starch | Colloid formation at room temperature | Photosensitive optoelectronic devices | Senapati and Sarkar (2015) |
| ZnS nanoparticles | Cubic agglomerated nanostructures | $ZnCl_2$, $Na_2S.H_2O$ | Wet chemical co-precipitation method | Solid state lighting, imaging, and other photonic devices | Balavijayalakshmi and Manju (2016) |
| Glucose capped ZnS nanoparticles | Average nanosize 8.35 nm predominantly spherical | Aqueous crude extract of *Stevia rebaudiana* and $Na_2S$ | Biological reduction, Reflux at 37 °C for 48 h | Cytotoxic effects of the nanoparticles against the MCF-7 cancer cell line | Alijani et al. (2019) |
| ZnS nanoparticles | Nanosized crystals spherically aggregated | Zinc acetate and thioacetamide | Heated 3 h at 85 °C | Showed higher antioxidant, antibacterial and antifungal behavior | Labiadh et al. (2016) |
| L-cysteine and mercaptopropionic-acid-capped ZnS | Nanosized 3.11 nm homogenously distributed spheres | Zn $(OAc)_2$, L-cys, MPA | One-pot aqueous phase synthesis method | Ratiometric fluorescence sensors and multicolor bioimaging | Ren et al. (2018) |
| ZnTe/CdSe core/shell QDs | 5.3 nm nanosructures | ($ZnEt_2$,CdO, selenium powder, tellurium powder | Hot injection at 270 °C to prepare ZnTe core, and around 240 °C to prepare the CdSe shell | Sensitizers in the construction of quantum dot sensitized solar cells (QDSCs) | Zhang et al. (2012) |
| ZnTe semiconductor nanoparticle | Nanosized cubic structure with average particle size of 6 nm | [$ZnSO_4.7H_2O$], $ZnCl_2$, [$Zn(NO_3)_2.6H_2O$] as Zn source, tellurium powder and $NaBH_4$ | Chemical precipitation method at ambient condition | Field-effect transistors and photodetectors | Jiang et al. (2010) |
| ZnTe nanosphere | Hollow nanospheres with crystalline and porous structure | $ZnCl_2$, tellurium powder, KOH solution, hydrazine monohydrate | Hydrothermal method | Electrocatalyst material for water oxidation | Dantas et al. (2012) |
| ZnTe/ZnO core–shell nanorods | Hetero-nanostructure | $Zn(NO_3)_2{\cdot}6H_2O$, $(CH_2)_6N_4$, (HTMA), $Na_2TeO_3$, $NaBH_4$ | Double hydrothermal method | p–n heterojunction structures for $H_2S$-gas sensing | Fang et al. (2009) |
| ZnTe thin films | Polycrystalline thin films with rough surface | ZnTe powder, deposited on tantalum silica substrates | Thermal deposition of thin film at different angles (0°, 20°, 40°, 60°, and 80°) | Solid-state electronic devices like LEDs, photodetectors and photovoltaic cells | Saikia et al. (2013a) |

## 5 Conclusion and future prospective

Zinc chalcogenide nanostructures, including quantum dots of ZnS, ZnSe, and ZnTe, can assume various forms, such as nanowires, nanorods, nanobelts, thin films, and spherical nanocrystals. Key factors like capping agents, reaction temperature, and reactant concentration are crucial in producing nanostructures with desirable morphology, porous characteristics, UV-to-visible absorbance, and strong luminescent properties. Additionally, methods involving Zn-rich alloy films and doping with transition metals have been employed to enhance their functionality. Despite some progress, research on core/shell heterostructures like ZnO/ZnSe and aqueous soluble nanostructures for biomedical purposes remains relatively limited,

offering ample opportunities for future exploration, particularly in the realm of nanocomposite materials. While ZnS nanostructures have been relatively easier to fabricate, the conditions for ZnSe and ZnTe nanostructures tend to be more challenging. These chalcogenide nanostructures find application in optoelectronic devices, optical and biosensing, photocatalysis, and cells such as photovoltaic and photoelectrochemical, with growing interest in their utilization in solar cells. Looking forward, considerable potential exists for leveraging the biocompatibility, cost-effectiveness, and non-toxic nature of zinc chalcogenide quantum dots in a myriad of biomedical applications. Continued research in this area could lead to significant advances in fields such as drug delivery, bioimaging, and biosensing.

## Author contributions

AC: Conceptualization, Data curation, Formal Analysis, Funding acquisition, Investigation, Methodology, Project administration, Resources, Supervision, Validation, Writing–original draft, Writing–review and editing. GK: Formal Analysis, Investigation, Writing–review and editing. GR: Writing–review and editing. HD: Investigation, Writing–review and editing. GJ: Formal Analysis, Writing–review and editing. TR: Data curation, Supervision, Writing–review and editing.

## Funding

The authors declare that no financial support was received for the research, authorship, and/or publication of this article.

## Acknowledgments

The authors gratefully acknowledge Raghu Engineering College Visakhapatnam for their support in every aspect.

## Conflict of interest

The authors declare that the research was conducted in the absence of any commercial or financial relationships that could be construed as a potential conflict of interest.

## Publisher's note

All claims expressed in this article are solely those of the authors and do not necessarily represent those of their affiliated organizations, or those of the publisher, the editors and the reviewers. Any product that may be evaluated in this article, or claim that may be made by its manufacturer, is not guaranteed or endorsed by the publisher.

## References

Alijani, H. Q., Pourseyedi, S., Mahani, M. T., and Khatami, M. (2019). Green synthesis of zinc sulfide (ZnS) nanoparticles using Stevia rebaudiana Bertoni and evaluation of its cytotoxic properties. *J. Mol. Struct.* 1175, 214–218. doi:10.1016/j.molstruc.2018.07.103

Anand, K. V., Chinnu, M. K., Kumar, R. M., Mohan, R., and Jayavel, R. (2009). Formation of zinc sulfide nanoparticles in HMTA matrix. *Appl. Surf. Sci.* 255 (21), 8879–8882. doi:10.1016/j.apsusc.2009.06.070

Ashwini, K., Pandurangappa, C., Avinash, K., Srinivasan, S., and Stefanakos, E. (2020). Synthesis, characterization and photoluminescence studies of samarium doped zinc sulfide nanophosphors. *J. Luminescence* 221, 117097. doi:10.1016/j.jlumin.2020.117097

Assadullah, I., Zaman, M. B., Malik, K. A., Malik, J. H., Bhat, A. A., and Tomar, R. (2021). Growth and properties of hydrothermally derived crystalline ZnSe quantum dots. *Environ. Sci. Pollut. Res.* 28, 3953–3959. doi:10.1007/s11356-020-11026-1

Azad Malik, M., Zulu, M., O'Brien, P., and Wakefield, t. l. G. (1998). Single-source molecular precursors for the deposition of zinc selenide quantum dots. *J. Mat. Chem.* 8 (8), 1885–1888. doi:10.1039/A802705F

Azzazy, H. M., Mansour, M. M., and Kazmierczak, S. C. (2007). From diagnostics to therapy: prospects ofquantumdots. *Clin. Biochem.* 40 (13-14), 917–927. doi:10.1016/j.clinbiochem.2007.05.018

Balavijayalakshmi, J., and Manju, S. (2016). Investigation of structural, optical and morphological properties of copper doped zinc sulphide nanoparticles. *Mat. Sci. Semicond. process.* 48, 101–105. doi:10.1016/j.mssp.2016.03.019

Biju, V., Itoh, T., Anas, A., Sujith, A., and Ishikawa, M. (2008). Semiconductor quantum dots and metalnanoparticles: syntheses, optical properties, and biological applications. *Anal. Bioanal. Chem.* 391, 2469–2495. doi:10.1007/s00216-008-2185-7

Bochev, B., and Yordanov, G. (2014). Room temperature synthesis of thioglycolate-coated zinc sulfide (ZnS) nanoparticles in aqueous medium and their physicochemical characterization. *Colloids Surf. A Physicochem. Eng. Asp.* 441, 84–90. doi:10.1016/j.colsurfa.2013.08.077

Bredol, M., and Merikhi, J. (1998). ZnS precipitation: morphology control. *J. Mat. Sci.* 33, 471–476. doi:10.1023/A:1004396519134

Cao, H., Xiao, Y., and Zhang, S. (2010). The synthesis and photocatalytic activity of ZnSe microspheres. *Nanotechnology* 22 (1), 015604. doi:10.1088/0957-4484/22/1/015604

Chang, J. H., Takai, T., Godo, K., Song, J. S., Koo, B. H., Hanada, T., et al. (2002). ZnTe-Based light-emitting-diodes grown on ZnTe substrates by molecular beam epitaxy. *Phys. Status Solidi B* 229 (2), 995–999. doi:10.1002/1521-3951(200201)229:2<995::AID-PSSB995>3.0.CO;2-G

Charvet, N., Reiss, P., Roget, A., Dupuis, A., Grünwald, D., Carayon, S., et al. (2004). Biotinylated CdSe/ZnSe nanocrystals for specific fluorescent labeling. *J. Mat. Chem.* 14(17), 2638–2642. doi:10.1039/B403714F

Chatterjee, A., Mondal, G., Guthikonda, K. K., and Saha, A. (2021). Aqueous synthesis of mercaptopropionic acid capped ZnSe QDs and investigation of photoluminescence properties with metal doping. *J.Indian Chem. Soc.* 98 (12), 100254. doi:10.1016/j.jics.2021.100254

Chatterjee, A., Priyam, A., Bhattacharya, S. C., and Saha, A. (2007a). pH dependent interaction of biofunctionalized CdS nanoparticles with nucleobases and nucleotides: a fluorimetric study. *J. Lumin.* 126 (2), 764–770. doi:10.1016/j.jlumin.2006.11.010

Chatterjee, A., Priyam, A., Bhattacharya, S. C., and Saha, A. (2007b). Differential growth and photoluminescence of ZnS nanocrystals with variation of surfactant molecules. *Colloids Surf. A Physicochem. Eng. Asp.* 297 (1-3), 258–266. doi:10.1016/j.colsurfa.2006.10.053

Chatterjee, A., Priyam, A., Das, S. K., and Saha, A. (2006). Size tunable synthesis of cysteine-capped CdS nanoparticles by γ-irradiation. *J. Colloid Interface Sci.* 294 (2), 334–342. doi:10.1016/j.jcis.2005.07.031

Chatterjee, A., Priyam, A., Ghosh, D., Mondal, S., Bhattacharya, S. C., and Saha, A. (2012). Interaction of ZnS nanoparticles with flavins and glucose oxidase: a fluorimetric investigation. *J. Lumin.* 132 (3), 545–549. doi:10.1016/j.jlumin.2011.08.034

Chen, P., Xiao, T. Y., Li, H. H., Yang, J. J., Wang, Z., Yao, H. B., et al. (2012). Nitrogen-doped graphene/ZnSe nanocomposites: hydrothermal synthesis and their enhanced electrochemical and photocatalytic activities. *ACS Nano* 6 (1), 712–719. doi:10.1021/nn204191x

Cheng, D. C., Hao, H. C., Zhang, M., Shi, W., and Lu, M. (2013). Improving Si solar cell performance using Mn: ZnSe quantum dot-doped PLMA thin film. *Nanoscale Res. Lett.* 8, 291–295. doi:10.1186/1556-276X-8-291

Chestnoy, N., Hull, R., and Brus, L. E. (1986). Higher excited electronic states in clusters of ZnSe, CdSe, and ZnS: spin-orbit, vibronic, and relaxation phenomena. *J. Chem. Phys.* 85 (4), 2237–2242. doi:10.1063/1.451119

Colli, A., Hofmann, S., Ferrari, A. C., Ducati, C., Martelli, F., Rubini, S., et al. (2005). Low-temperature synthesis of ZnSe nanowires and nanosaws by catalyst-assisted molecular-beam epitaxy. *Appl. Phys. Lett.* 11 (15), 86. doi:10.1063/1.1897053

C Sharma, D., Vijay, K., Yk Sharma, Y., and Srivastava, S. (2013). Preparation and characterization of the chromium doped ZnTe thin films. *Adv. Mat. Lett.* 4 (1), 68–70. doi:10.5185/amlett.2013.icnano.118

Dantas, N. O., dos Santos Silva, A., da Silva, S. W., de Morais, P. C., Pereira-da-Silva, M. A., and Marques, G. E. (2010). ZnTe nanocrystal formation and growth control on UV-transparent substrate. *Chem. Phys. Lett.* 500 (1-3), 46–48. doi:10.1016/j.cplett.2010.09.035

Dantas, N. O., Silva, A. S., Neto, E. S., and Lourenço, S. A. (2012). Thermal activated energy transfer between luminescent states of $Mn^{2+}$doped ZnTe nanoparticles embedded in a glass matrix. *Phys. Chem. Chem. Phys.* 14 (10), 3520–3529. doi:10.1039/C2CP23681H

Deng, Z., Pal, S., Samanta, A., Yan, H., and Liu, Y. (2013). DNA functionalization of colloidal II–VI semiconductor nanowires for multiplex nano heterostructures. *Chem. Sci.* 4(5), 2234–2240. doi:10.1039/C3SC00065F

Deng, Z., Qi, J., Zhang, Y., Liao, Q., and Huang, Y. (2007). Growth mechanism and optical properties of ZnS nanotetrapods. *Nanotechnology* 18 (47), 475603. doi:10.1088/0957-4484/18/47/475603

Dhas, N. A., Zaban, A., and Gedanken, A. (1999). Surface synthesis of zinc sulfide nanoparticles on silica microspheres: sonochemical preparation, characterization, and optical properties. *Chem. Mat.* 11 (3), 806–813. doi:10.1021/cm980670s

Dhungana, S., Paudel, B. R., and Gautam, S. K. (2016). Synthesis and characterization of ZnTe nanoparticles. *Nepal J. Sci. Technol.* 17 (1), 1–3. doi:10.3126/njst.v17i1.25054

Du, J., Xu, L., Zou, G., Chai, L., and Qian, Y. (2006). Solvothermal synthesis of single crystalline ZnTe nanorod bundles in a mixed solvent of ethylenediamine and hydrazine hydrate. *J. Cryst. Growth.* 291 (1), 183–186. doi:10.1016/j.jcrysgro.2006.02.040

Duan, X., Huang, Y., Agarwal, R., and Lieber, C. M. (2003). Single-nanowire electrically driven lasers. *Nature* 421 (6920), 241–245. doi:10.1038/nature01353

Dunpall, R., Mlowe, S., and Revaprasadu, N. (2014). Evidence of oriented attachment in the growth of functionalized ZnTe nanoparticles for potential applications in bio-imaging. *New J. Chem.* 38(12), 6002–6007. doi:10.1039/C4NJ01183J

Dwivedi, D. K., and Dubey, M. (2009). Synthesis, characterization and electrical properties of znte nanoparticles. *J. Ovonic Res.* (2), 5. doi:10.4236/wjnse.2016.63012

Ebrahimi, S., and Yarmand, B. (2019). Morphology engineering and growth mechanism of ZnS nanostructures synthesized by solvothermal process. *J. Nanopart Res.* 21, 1–12. doi:10.1007/s11051-019-4714-z

Ersching, K., Faita, F. L., Campos, C. E., Grandi, T. A., and Pizani, P. S. (2010). Ageing effect on mechanically alloyed ZnTe nanocrystals. *J. Alloys Compd.* 493 (1-2), 294–298. doi:10.1016/j.jallcom.2009.12.083

Fang, X., Bando, Y., Liao, M., Gautam, U. K., Zhi, C., Dierre, B., et al. (2009). Single-crystalline ZnS nanobelts as ultraviolet-light sensors. *Adv. Mat.* 21 (20), 2034–2039. doi:10.1002/adma.200802441

Feng, L., Mao, D., Tang, J., Collins, R. T., and Trefny, J. U. (1996). The structural, optical, and electrical properties of vacuum evaporated Cu-doped ZnTe polycrystalline thin films. *J. Electron. Mat.* 25, 1422–1427. doi:10.1007/BF02655377

Feng, X., Singh, K., Bhavanam, S., Palekis, V., Morel, D. L., and Ferekides, C. (2013). Preparation and characterization of ZnTe as an interlayer for CdS/CdTe substrate thin film solar cells on flexible substrates. *Thin Solid Films* 535, 202–205. doi:10.1016/j.tsf.2012.11.103

Fu, H., Li, H., Jie, W., and Yang, L. (2006). The growth and characterization of ZnSe nanoneedles by a simple chemical vapor deposition method. *J. Cryst. Growth* 289 (2), 440–444. doi:10.1016/j.jcrysgro.2005.11.098

Gao, J., Chen, K., Xie, R., Xie, J., Yan, Y., Cheng, Z., et al. (2010). *In vivo* tumor-targeted fluorescence imaging using near-infrared non-cadmium quantum dots. *Bioconjugate Chem.* 21 (4), 604–609. doi:10.1021/bc900323v

Gao, X., Cui, Y., Levenson, R. M., Chung, L. W., and Nie, S. (2004). *In vivo* cancer targeting and imaging with semiconductor quantum dots. *Nat. Biotechnol.* 22 (8), 969–976. doi:10.1038/nbt994

Gates, B., Mayers, B., Cattle, B., and Xia, Y. (2002). Synthesis and characterization of uniform nanowires of trigonal selenium. *Adv. Funct. Mat.* 12 (3), 219–227. doi:10.1002/1616-3028(200203)12:3<219::AID-ADFM219>3.0.CO;2-U

Gessert, T. A., Mason, A. R., Reedy, R. C., Matson, R., Coutts, T. J., and Sheldon, P. (1995). Development of rf sputtered, Cu-doped ZnTe for use as a contact interface layer to p-CdTe. *J. Electron. Mat.* 24, 1443–1449. doi:10.1007/BF02655462

Ghosh, S., Ghosh, D., Bag, P. K., Bhattacharya, S. C., and Saha, A. (2011). Aqueous synthesis of ZnTe/dendrimer nanocomposites and their antimicrobial activity: implications in therapeutics. *Nanoscale* 3 (3), 1139–1148. doi:10.1039/C0NR00610F

Gudiksen, M. S., Wang, J., and Lieber, C. M. (2001). Synthetic control of the diameter and length of single crystal semiconductor nanowires. *J. Phys. Chem. B* 105 (19), 4062–4064. doi:10.1021/jp010540y

Hao, J., Liu, H., Miao, J., Lu, R., Zhou, Z., Zhao, B., et al. (2019). A facile route to synthesize CdSe/ZnS thick-shell quantum dots with precisely controlled greenemission properties: towards QDs based LED applications. *Sci. Rep.* 9 (1), 12048. doi:10.1038/s41598-019-48469-7

He, Y., Sai, L. M., Lu, H. T., Hu, M., Lai, W. Y., Fan, Q. L., et al. (2007). Microwave-assisted synthesis of water-dispersed CdTe nanocrystals with high luminescent efficiency and narrow size distribution. *Chem. Mat.* 19 (3), 359–365. doi:10.1021/cm061863f

Hieu, N. M., Hien, T. T., Chinh, N. D., Quang, N. D., Hung, N. M., Van Phuoc, C., et al. (2020). ZnTe-coated ZnO nanorods: hydrogen sulfide nano-sensor purely controlled by pn junction. *Mater Des.* 191, 108628. doi:10.1016/j.matdes.2020.108628

Hossain, M. S., Islam, R., and Khan, K. A. (2008a). Electrical conduction mechanisms of undoped and vanadium doped ZnTe thin films. *Chalcogenide Lett.* 5 (1), 1–9.

Hossain, M. S., Islam, R., and Khan, K. A. (2008b). Temperature effect on the electrical properties of undoped and vanadium-doped ZnTe thin films. *Renew. Energy.* 33 (4), 642–647. doi:10.1016/j.renene.2007.04.003

Hou, D. D., Wu, H., and Liu, Y. K. (2010). Preparation of ultrawide ZnSe nanoribbons with the function of lasing cavity. *Optoelectron. Lett.* 6 (4), 241–244. doi:10.1007/s11801-010-0030-7

Hou, L., Zhang, Q., Ling, L., Li, C. X., Chen, L., and Chen, S. (2013). Interfacial fabrication of single-crystalline ZnTe nanorods with high blue fluorescence. *J. Am. Chem. Soc.* 135 (29), 10618–10621. doi:10.1021/ja4047476

Hussain, T., Al-Kuhaili, M. F., Durrani, S. M., and Qayyum, H. A. (2018). Influence of angle deposition on the properties of ZnTe thin films prepared by thermal evaporation. *Ceram. Int.* 44 (9), 10130–10140. doi:10.1016/j.ceramint.2018.02.232

HusseinP, H. F. (2013). Preperation and study optical trasnpraency of spray deposted ZnS films with different annealing temperatures. *J. Basrah Res.* 39 (4).

Ilanchezhiyan, P., Kumar, G. M., Xiao, F., Madhankumar, A., Siva, C., Yuldashev, S. U., et al. (2018). Interfacial charge transfer in ZnTe/ZnO nano arrayed heterostructures and their improved photoelectronic properties. *Sol. Energy Mater Sol. Cells* 183, 73–81. doi:10.1016/j.solmat.2018.04.010

Imran, M., Ashraf, W., Hafiz, A. K., and Khanuja, M. (2022). Synthesis and performance analysis of photocatalytic activity of $ZnIn_2S_4$ microspheres synthesized using a low-temperature method. *ACS Omega* 7, 22987–22996. doi:10.1021/acsomega.2c00945

Jen-La Plante, I., Zeid, T. W., Yang, P., and Mokari, T. (2010). Synthesis of metal sulfide nanomaterials via thermal decomposition of single-source precursors. *J. Mat. Chem.* 20(32), 6612–6617. doi:10.1039/C0JM00439A

Jiang, C., Zhang, W., Zou, G., Yu, W., and Qian, Y. (2005). Synthesis and characterization of ZnSe hollow nanospheres via a hydrothermal route. *Nanotechnology* 16 (4), 551–554. doi:10.1088/0957-4484/16/4/036

Jiang, F., Li, Y., Ye, M., Fan, L., Ding, Y., and Li, Y. (2010). Ligand-tuned shape control, oriented assembly, and electrochemical characterization of colloidal ZnTe nanocrystals. *Chem. Mat.* 22 (16), 4632–4641. doi:10.1021/cm101225b

Jiang, Y., Meng, X. M., Liu, J., Hong, Z. R., Lee, C. S., and Lee, S. T. (2003). ZnS nanowires with wurtzite polytype modulated structure. *Adv. Mat.* 15 (14), 1195–1198. doi:10.1002/adma.200304852

Jiao, S., Shen, Q., Mora-Seró, I., Wang, J., Pan, Z., Zhao, K., et al. (2015). Band engineering in core/shell ZnTe/CdSe for photovoltage and efficiency enhancement in exciplex quantum dot sensitized solar cells. *ACS Nano* 9 (1), 908–915. doi:10.1021/nn506638n

Joo, J., Na, H. B., Yu, T., Yu, J. H., Kim, Y. W., Wu, F., et al. (2003). Generalized and facile synthesis of semiconducting metal sulfide nanocrystals. *J. Am. Chem. Soc.* 125 (36), 11100–11105. doi:10.1021/ja0357902

Jubeer, E. M., Manthrammel, M. A., Shkir, M., Subha, P. A., Yahia, I. S., and Alfaify, S. A. (2021). Microwave assisted synthesis of quantum dots like ZnS nanoparticles for optoelectronic applications: an effect of CTAB concentrations. *Optik* 240, 166812. doi:10.1016/j.ijleo.2021.166812

Jun, Y. W., Choi, C. S., and Cheon, J. (2001). Size and shape controlled ZnTe nanocrystals with quantum confinement effect. *ChemComm* (1), 101–102. doi:10.1039/B008376N

Jun, Y. W., Koo, J. E., and Cheon, J. (2000). One-step synthesis of size tuned zinc selenide quantum dots via a temperature controlled molecular precursor approach. *ChemComm* 14, 1243–1244. doi:10.1039/B002983L

Kaito, C., Saito, Y., and Fujita, K. (1987). A new preparation method of ultrafine particles of metallic sulfides. *JJAP 1* 26 (12A), L1973. doi:10.1143/JJAP.26.L1973

Kar, S., Biswas, S., and Chaudhuri, S. (2005). Catalytic growth and photoluminescence properties of ZnS nanowires. *Nanotechnol.* 16 (6), 737–740. doi:10.1088/0957-4484/16/6/018

Karanikolos, G. N., Alexandridis, P., Itskos, G., Petrou, A., and Mountziaris, T. J. (2004). Synthesis and size control of luminescent ZnSe nanocrystals by a Microemulsion– gas contacting technique. *Langmuir.* 20 (3), 550–553. doi:10.1021/la035397+

Kim, D. J., Kim, J. W., Kim, E. J., and Koo, K. K. (2011). Formation of 1-D ZnTe nanocrystals by aerosol-assisted spray pyrolysis. *Korean J. Chem. Eng.* 28, 1120–1125. doi:10.1007/s11814-010-0458-2

Kole, A. K., and Kumbhakar, P. (2012). Cubic-to-hexagonal phase transition and optical properties of chemically synthesized ZnS nanocrystals. *Results Phys.* 2, 150–155. doi:10.1016/j.rinp.2012.09.010

Labiadh, H., Lahbib, K., Hidouri, S., Touil, S., and Chaabane, T. B. (2016). Insight of ZnS nanoparticles contribution in different biological uses. *Asian pac. J. Trop. Med.* 9 (8), 757–762. doi:10.1016/j.apjtm.2016.06.008

Li, Y., Ding, Y., and Wang, Z. (1999). A novel chemical route to ZnTe semiconductor nanorods. *Adv. Mat.* 11 (10), 847–850. doi:10.1002/(SICI)1521-4095(199907)11:10<847::AID-ADMA847>3.0.CO;2-B

Lin, B., Li, S., Hou, X., and Li, H. (2015)). Preparation of high performance mullite ceramics from high-aluminum fly ash by an effective method. *J. Alloys Compd.* 623, 359–361. doi:10.1016/j.jallcom.2014.11.023

Lincheneau, C., Amelia, M., Oszajca, M., Boccia, A., D'Orazi, F., Madrigale, M., et al. (2014). Synthesis and properties of ZnTe and ZnTe/ZnS core/shell semiconductor nanocrystals. *J. Mat. Chem. C* 2(16):2877–2886. doi:10.1039/C3TC32385D

Liu, F., Xue, F., Si, Y., Chen, G., Guan, X., Lu, K., et al. (2021). Functionalized Cd0. 5Zn0. 5S chalcogenide nanotwins enabling Z-scheme photocatalytic water splitting. *ACS Appl. Nano Mater.* 4 (1), 759–768. doi:10.1021/acsanm.0c03054

Liu, M. T., and Li, W. (2018). Growth and optical property of PbS/ZnS nanocrystals. *Superlattices Microstruct.* 120, 727–731. doi:10.1016/j.spmi.2018.06.051

Liu, Z., Chen, G., Liang, B., Yu, G., Huang, H., Chen, D., et al. (2013). Fabrication of high-quality ZnTe nanowires toward high-performance rigid/flexible visible-light photodetectors. *Opt. express* 21 (6), 7799–7810. doi:10.1364/OE.21.007799

Löffler, T., Hahn, T., Thomson, M., Jacob, F., and Roskos, H. G. (2005). Large-area electro-optic ZnTe terahertz emitters. *Opt. express* 13 (14), 5353–5362. doi:10.1364/OPEX.13.005353

Lu, H. Y., Chu, S. Y., and Tan, S. S. (2004). The characteristics of low-temperature-synthesized ZnS and ZnO nanoparticles. *Cryst. Growth* 269 (2-4), 385–391. doi:10.1016/j.jcrysgro.2004.05.050

Luo, S., He, X., Shen, H., Li, J., Yin, X., Oron, D., et al. (2017). Vertically aligned ZnO/ZnTe core/shell heterostructures on an AZO substrate for improved photovoltaic performance. *RSC Adv.* 7(24), 14837–14845. doi:10.1039/C6RA27641E

Mai, X., Thi Bui, D., Pham, D., Bui, T., Nguyen, T. M., Oh, J., et al. (2018). *American Journal of Engineering Research (AJER) e.* USA: ISSN, 27–32. 2320-0847 p-ISSN : 2320-0936. 7,6.

Medintz, I. L., Uyeda, H. T., Goldman, E. R., and Mattoussi, H. (2005). Quantum dot bioconjugates for imaging, labelling and sensing. *Nat. Mat.* 4 (6), 435–446. doi:10.1038/nmat1390

Michalet, X., Pinaud, F. F., Bentolila, L. A., Tsay, J. M., Doose, S. J., Li, J. J., et al. (2005). Quantum dots for live cells, *in vivo* imaging, and diagnostics. *science* 307 (5709), 538–544. PMID: 15681376; PMCID: PMC1201471. doi:10.1126/science.1104274

Mntungwa, N., Pullabhotla, V. S., and Revaprasadu, N. (2012). A facile hybrid route to luminescent ZnTe nanoparticles. *Mat. Lett.* 81, 108–111. doi:10.1016/j.matlet.2012.04.131

Moon, H., Nam, C., Kim, C., and Kim, B. (2006). Synthesis and photoluminescence of zinc sulfide nanowires by simple thermal chemical vapor deposition. *Mat. Res. Bull.* 41 (11), 2013–2017. doi:10.1016/j.materresbull.2006.04.007

Murray, C. B., Kagan, C. R., and Bawendi, M. G. (2000). Synthesis and characterization of monodisperse nanocrystals and close-packed nanocrystal assemblies. *Annu. Rev. Mat. Sci.* 30 (1), 545–610. doi:10.1146/annurev.matsci.30.1.545

Mussa Farkhani, S., and Valizadeh, A. (2014). Review: three synthesis methods of CdX (X = Se, S or Te) quantum dots. *IET nanobiotechnology* 8 (2), 59–76. doi:10.1049/iet-nbt.2012.0028

Naeimi, H., Kiani, F., and Moradian, M. (2014). ZnS nanoparticles as an efficient and reusable heterogeneous catalyst for synthesis of 1-substituted-1 H-tetrazoles under solvent-free conditions. *J. Nanoparticle Res.* 16, 2590–2599. doi:10.1007/s11051-014-2590-0

Nithyaprakash, D., Ramamurthy, M., Thirunavukarasu, P., Balasubramaniam, T., Chandrasekaran, J., and Maadeswaran, P. (2009). Effect of substrate temperature on structural, optical and thermal properties of chemically sprayed ZnS thin films. *J. Optoelectron Biome1* 1, 42–51.

Norberg, N. S., Parks, G. L., Salley, G. M., and Gamelin, D. R. (2006). Giant excitonic Zeeman splittings in colloidal $Co^{2+}$-doped ZnSe quantum dots. *J. Am. Chem. Soc. Soc.* 128 (40), 13195–13203. doi:10.1021/ja063425f

Norris, D. J., Yao, N., Charnock, F. T., and Kennedy, T. A. (2001). High-quality manganese-doped ZnSe nanocrystals. *Nano Lett.* 1 (1), 3–7. doi:10.1021/nl005503h

Omata, T., Tsukuda, S., and Asano, H. (2019). 81-1: *invited paper:* quantum dot phosphors containing none of hazardous element; ZnTe-based alloy quantum dots. *SID Symposium Dig. Tech. Pap. 2019* 50 (1), 1160–1163. doi:10.1002/sdtp.13136

Onwudiwe, D. C., and Ajibade, P. A. (2011). ZnS, CdS and HgS nanoparticles via alkyl-phenyl dithiocarbamate complexes as single source precursors. *Int. J. Mol. Sci.* 12 (9), 5538–5551. doi:10.3390/ijms12095538

Park, J., Dvoracek, C., Lee, K. H., Galloway, J. F., Hyo-eun, C. B., Pomper, M. G., et al. (2011)). CuInSe/ZnS core/shell NIR quantum dots for biomedical imaging. *Small* 7 (22), 3148–3152. doi:10.1002/smll.201101558

Priyam, A., Chatterjee, A., Bhattacharya, S. C., and Saha, A. (2009). Conformation and activity dependent interaction of glucose oxidase with CdTequantum dots: towards developing a nanoparticle based enzymatic assay. *Photochem. Photobiol. Sci.* 8, 362–370. doi:10.1039/B815881A

Priyam, A., Chatterjee, A., Das, S. K., and Saha, A. (2005). Size dependent interaction of biofunctionalized CdS nanoparticles with tyrosine at different pH. *ChemComm* (32), 4122–4124. doi:10.1039/B505960G

Promnopas, W., Thongtem, T., and Thongtem, S. (2014). ZnTe semiconductor-polymer gel composited electrolyte for conversion of solar energy. *J. Nanomater.* 2014, 1–6. doi:10.1155/2014/529629

Qian, H., Qiu, X., Li, L., and Ren, J. (2006). Microwave-assisted aqueous synthesis: a rapid approach to prepare highly luminescent ZnSe (S) alloyed quantum dots. *J. Phys. Chem. B* 110 (18), 9034–9040. doi:10.1021/jp0539324

Ramamoorthy, C., and Rajendran, V. (2018). Formation of solid and hollow sphere ZnS nanoparticles by hydrothermal process and their structural, optical and photocatalytic activity. *Appl. Phys. A* 124, 500–508. doi:10.1007/s00339-018-1851-7

Ren, Y., Wang, Y., Yang, M., Liu, E., Hu, X., Zhang, X., et al. (2018). Aqueous synthesis of L-cysteine and mercaptopropionic acid co-capped ZnS quantum dots with dual emissions. *Nanotechnology* 29 (30), 305707. doi:10.1088/1361-6528/aac124

Routkevitch, D., Bigioni, T., Moskovits, M., and Xu, J. M. (1996). Electrochemical fabrication of CdS nanowire arrays in porous anodic aluminum oxide templates. *J. Phys. Chem.* 100 (33), 14037–14047. doi:10.1021/jp952910m

Sadaqat, M., Nisar, L., Hussain, F., Ashiq, M. N., Shah, A., Ehsan, M. F., et al. (2019). Zinc-telluride nanospheres as an efficient water oxidation electrocatalyst displaying a low overpotential for oxygen evolution. *J. Mat. Chem.A.* 7 (46), 26410–26420. doi:10.1039/C9TA07171G

Saikia, K., Deb, P., and Kalita, E. (2013a). Facile synthesis of highly luminescent ZnSe (S) alloyed quantum dot for biomedical imaging. *Curr. Appl. Phys.* 13 (5), 925–930. doi:10.1016/j.cap.2013.01.042

Saikia, K., Deb, P., and Kalita, E. (2013b). Sensitive fluorescence response of ZnSe (S) quantum dots: an efficient fluorescence probe. *Phys. Screen.* 87 (6), 065802. doi:10.1088/0031-8949/87/06/065802

Salem, A., Saion, E., Al-Hada, N. M., Shaari, A. H., Kamari, H. M., Soltani, N., et al. (2016). Formation of a colloidal CdSe and ZnSe quantum dots via a gamma radiolytic technique. *Appl. Sci.* 6 (10), 278. doi:10.3390/app6100278

Sánchez-López, J. C., Justo, A., and Fernandez, A. (1999). Tailored preparation of quantum-sized ZnS nanoparticles by the gas-phase condensation method. *Langmuir* 15 (22), 7822–7828. doi:10.1021/la981718j

Sapsford, K. E., Pons, T., Medintz, I. L., and Mattoussi, H. (2006). Biosensing with luminescent semiconductor quantum dots. *Sensors* 6 (8), 925–953. doi:10.3390/s6080925

Selvaraj, J., Mahesh, A., Asokan, V., Baskaralingam, V., Dhayalan, A., and Paramasivam, T. (2017). Phosphine-Free, highly emissive, water-soluble Mn:ZnSe/ZnS core–shell nanorods: synthesis, characterization, and *in vitro* bioimaging of HEK293 and HeLa cells. *ACS Appl. Nano Mater* 1 (1), 371–383. doi:10.1021/acsanm.7b00218

Senapati, U. S., and Sarkar, D. (2015). Synthesis and characterization of biopolymer protected zinc sulphide nanoparticles. *Superlattices Microstruct.* 85, 722–733. doi:10.1016/j.spmi.2015.06.040

Senthilkumar, K., Ramamurthi, K., Kalaivani, T., and Balasubramanian, V. (2013). Low temperature synthesis of MPA capped ZnS quantum dots and its characterization studies. *Ind. J. Adv. Chem. Sci.* 2 (1), 1–5.

Shao, P., Wang, H., Zhang, Q., and Li, Y. (2011). White light emission from Mn-doped ZnSe d-dots synthesized continuously in microfluidic reactors. *J. Mat. Chem.* 21 (44), 17972–17977. doi:10.1039/C1JM12128F

Sharifi, F., Sharififar, F., Sharifi, I., Alijani, H. Q., and Khatami, M. (2018). Cytotoxicity, leishmanicidal, and antioxidant activity of biosynthesised zinc sulphide nanoparticles using Phoenix dactylifera. *IET Nanobiotechnology* 12 (3), 264–269. doi:10.1049/iet-nbt.2017.0204

Shavel, A., Gaponik, N., and Eychmüller, A. (2004). Efficient UV-blue photoluminescing thiol-stabilized water-soluble alloyed ZnSe (S) nanocrystals. *J. Phys. Chem.B.* 13 (19), 5905–5908. doi:10.1021/jp037941t

Shaygan, M., Gemming, T., Bezugly, V., Cuniberti, G., Lee, J. S., and Meyyappan, M. (2014). *In situ* observation of melting behavior of ZnTe nanowires. *J. Phys. Chem. C* 118 (27), 15061–15067. doi:10.1021/jp503312z

Shkir, M., Aarya, S., Singh, R., Arora, M., Bhagavannarayana, G., and Senguttuvan, T. D. (2012). Synthesis of ZnTe nanoparticles by microwave irradiation technique, and their characterization. *Nanosci. Nanotechnol. Lett.* 4(4):405–408. doi:10.1166/nnl.2012.1328

Singhal, M., Sharma, J. K., Jeon, H. C., Kang, T. W., and Kumar, S. (2019). Synthesis and characterisation of functional manganese doped ZnS quantum dots for bio-imaging application. *Adv. Appl. Ceram.* 118 (6), 321–328. doi:10.1080/17436753.2019.1587937

Smith, B. R., Cheng, Z., De, A., Koh, A. L., Sinclair, R., and Gambhir, S. S. (2008). Real-time intravital imaging of RGD– quantum dot binding to luminal endothelium in mouse tumor neovasculature. *Nano Lett.* 10 (9), 2599–2606. doi:10.1021/nl080141f

Späth, B., Fritsche, J., Säuberlich, F., Klein, A., and Jaegermann, W. (2005). Studies of sputtered ZnTe films as interlayer for the CdTe thin film solar cell. *Thin Solid Films* 480, 204–207. doi:10.1016/j.tsf.2004.11.073

Stanić, V., Etsell, T. H., Pierre, A. C., and Mikula, R. J. (1997). Sol-gel processing of ZnS. *Mat. Lett.* 31 (1-2), 35–38. doi:10.1016/S0167-577X(96)00237-6

Tran, T. A., Krishnamoorthy, K., Cho, S. K., and Kim, S. J. (2016). Inhibitory effect of zinc sulfide nanoparticles towards breast cancer stem cell migration and invasion. *J. Biomed. Nanotechnol.* 12 (2), 329–336. doi:10.1166/jbn.2016.2187

Tuan, C. A., Yen, V. H., Cuong, K. C., Thuy, N. T. M., An, P. M., Ngoc, N. T. B., et al. (2021). Optical properties and energy transfer mechanism of Eu3+, Ce3+ doped and co-doped ZnS quantum dots. *J. Luminescence* 236, 118106. doi:10.1016/j.jlumin.2021.118106

Ueta, A., and Hommel, D. (2002). New concept for ZnTe-based homoepitaxial light-emitting diodes grown by molecular beam epitaxy. *Phys. Status Solidi A* 192 (1), 177–182. doi:10.1002/1521-396X(200207)192:1<177::AID-PSSA177>3.0.CO;2-8

Valizadeh, A., Mikaeili, H., Samiei, M., Farkhani, S. M., Zarghami, N., Kouhi, M., et al. (2012). Quantum dots: synthesis, bioapplications, and toxicity. *Nanoscale Res. Lett.* 7, 480–484. doi:10.1186/1556-276X-7-480

Wageh, S., Ling, Z. S., and Xu-Rong, X. (2003). Growth and optical properties of colloidal ZnS nanoparticles. *J. Cryst. Growth* 255 (3-4), 332–337. doi:10.1016/S0022-0248(03)01258-2

Wang, L., Xu, X., and Yuan, X. (2010). Preparation and photoluminescent properties of doped nanoparticles of ZnS by solid-state reaction. *J. Lumin.* 130 (1), 137–140. doi:10.1016/j.jlumin.2009.07.036

Wang, L. P., and Hong, G. Y. (2000). A new preparation of zinc sulfide nanoparticles by solid-state method at low temperature. *Mat. Res. Bull.* 35 (5), 695–701. doi:10.1016/S0025-5408(00)00261-0

Wang, Q. Y., Liu, J., Murugan, A. V., and Manthiram, A. (2009). High capacity double-layer surface modified Li [Li 0.2 Mn 0.54 Ni 0.13 Co 0.13] O 2 cathode with improved rate capability. *J. Mat. Chem.* 19(28), 4965–4972. doi:10.1039/B823506F

Wang, X., Xie, Z., Huang, H., Liu, Z., Chen, D., and Shen, G. (2012). Gas sensors, thermistor and photodetector based on ZnS nanowires. *J. Mat. Chem.* 22(14): 6845–6850. doi:10.1039/C2JM16523F

Xia, Y., Yang, P., Sun, Y., Wu, Y., Mayers, B., Gates, B., et al. (2003). One-dimensional nanostructures: synthesis, characterization, and applications. *Adv. Mat.* 15 (5), 353–389. doi:10.1002/adma.200390087

Xiong, S., Xi, B., Wang, C., Xi, G., Liu, X., and Qian, Y. (2007). Solution-phase synthesis and high photocatalytic activity of wurtzite ZnSe ultrathin nanobelts: a general route to 1D semiconductor nanostructured materials. *Chem. Eur. J.* 13 (28), 7926–7932. doi:10.1002/chem.200700334

Yan, H., Li, T., Lu, Y., Cheng, J., Peng, T., Xu, J., et al. (2016). Template-free synthesis of ordered ZnO@ZnS core–shell arrays for high performance supercapacitors. *Dalton Trans.* 45(44), 17980–17986. doi:10.1039/C6DT03435G

Yang, J., Zeng, J. H., Yu, S. H., Yang, L., Zhou, G. E., and Qian, Y. T. (2000). Formation process of CdS nanorods via solvothermal route. *Chem. Mat.* 12 (11), 3259–3263. doi:10.1021/cm0000144

Yang, L., Xie, R., Liu, L., Xiao, D., and Zhu, J. (2011). Synthesis and characterization of ZnSe nanocrystals by W/O reverse microemulsion method: the effect of cosurfactant. *J. Phys. Chem. C* 115 (40), 19507–19512. doi:10.1021/jp204798y

Yang, X., Liu, X., Liu, Z., Pu, F., Ren, J., and Qu, X. (2012). Near-infrared light-triggered, targeted drug delivery to cancer cells by aptamer gated nanovehicles. *Adv. Mat.Deerf. Beach, Fla.* 24 (21), 2890–2895. doi:10.1002/adma.201104797

Yin, G., Hong, J., and Xu, Z. (2004). Rapid fabrication and optical properties of zinc sulfide nanocrystallines in a heterogeneous system. *Mat. Res. Bull.* 39 (12), 1967–1972. doi:10.1016/j.materresbull.2004.01.011

Yong, K. T., Sahoo, Y., Zeng, H., Swihart, M. T., Minter, J. R., and Prasad, P. N. (2007). Formation of ZnTe nanowires by oriented attachment. *Chem. Mat.* 19 (17), 4108–4110. doi:10.1021/cm0709774

Yoshino, K., Memon, A., Yoneta, M., Ohmori, K., Saito, H., and Ohishi, M. (2002). Optical characterization of the ZnTe pure-green LED. *Phys. Status Solidi B* 229 (2), 977–980. doi:10.1002/1521-3951(200201)229:2<977::AID-PSSB977>3.0.CO;2-G

Yu, D., Wang, D., Meng, Z., Lu, J., and Qian, Y. (2002). Synthesis of closed PbS nanowires with regular geometric morphologiesElectronic supplementary information (ESI) available: XRD pattern of the PbS CNWs, FTIR spectrum of the polymer, TEM images of more PbS CNWs. *J. Mat. Chem.* 12(3), 403–405.doi:10.1039/B111187F

Yu, S. H., Yang, J., Wu, Y. S., Han, Z. H., Xie, Y., and Qian, Y. T. (1998). Hydrothermal preparation and characterization of rod-like ultrafine powders of bismuth sulfide. *Mat. Res. Bull.* 33 (11), 1661–1666. doi:10.1016/S0025-5408(98)00161-5

Zhai, T., Zhong, H., Gu, Z., Peng, A., Fu, H., Ma, Y., et al. (2007). Manipulation of the morphology of ZnSe sub-micron structures using CdSe nanocrystals as the seeds. *J. Phys. Chem. C* 111 (7), 2980–2986. doi:10.1021/jp067498x

Zhai, X., Zhang, X., Chen, S., Yang, W., and Gong, Z. (2012). Oleylamine as solvent and stabilizer to synthesize shape-controlled ZnS nanocrystals with good optical properties. *Colloids Surf. A Physicochem Eng. Asp.* 409, 126–129. doi:10.1016/j.colsurfa.2012.05.047

Zhang, J., Jin, S., Fry, H. C., Peng, S., Shevchenko, E., Wiederrecht, G. P., et al. (2011). Synthesis and characterization of wurtzite ZnTe nanorods with controllable aspect ratios. *J. Am. Chem. Soc.* 133 (39), 15324–15327. doi:10.1021/ja206309h

Zhang, W. H., Zhang, D., Zhang, R. J., Xia, F., and Liu, Y. F. (2012). Flow injection analysis of volatile phenols in environmental water samples using CdTe/ZnSe nanocrystals as a fluorescent probe. *Anal. Bioanal. Chem.* 402, 895–901. doi:10.1007/s00216-011-5477-2

Zhang, X. T., Liu, Z., Ip, K. M., Leung, Y. P., Li, Q., and Hark, S. K. (2004). Luminescence of ZnSe nanowires grown by metalorganic vapor phase deposition under different pressures. *J. Appl. Phys.* 95 (10), 5752–5755. doi:10.1063/1.1699497

Zhao, W. H., Wei, Z. Q., Wu, X. J., Zhang, X. D., Zhang, L., and Wang, X. (2019). Microstructure and photocatalytic activity of Ni-doped ZnS nanorods prepared by hydrothermal method. *Trans. Nonferrous Met. Soc. China* 29 (1), 157–164. doi:10.1016/S1003-6326(18)64924-6

Zhou, J., Zhuang, H. L., and Wang, H., Layered tetragonal zinc chalcogenides for energy-related applications: from photocatalysts for water splitting to cathode materials for Li-ion batteries. *Nanoscale*, 2017:9(44), pp.17303–17311. doi:10.1039/C7NR04289B

Zhu, J., Liu, S., Palchik, O., Koltypin, Y., and Gedanken, A. (2000). A novel sonochemical method for the preparation of nanophasic sulfides: synthesis of HgS and PbS nanoparticles. *J. Solid State Chem.* 153 (2), 342–348. doi:10.1006/jssc.2000.8780